Current Trends in Polymer Science
Vol. 17, 2016

Review

Polymeric dental composites based on remineralizing amorphous calcium phosphate fillers

Drago Skrtic[1,*] and Joseph M. Antonucci[2]

[1]Volpe Research Center, American Dental Association Foundation, Gaithersburg, MD 20899-8546; [2]Biomaterials Group, Biosystems and Biomaterials Division, National Institute of Standards and Technology, Gaithersburg, MD 20899-8543, USA.

ABSTRACT

For over two decades we have systematically explored structure-composition-property relationships of amorphous calcium phosphate (ACP)-based polymeric dental composites. The appeal of these bioactive materials stems from their intrinsic ability to prevent demineralization and/or restore defective tooth structures *via* sustained release of remineralizing calcium and phosphate ions. Due to the compositional similarity of the ACP to biological tooth mineral, ACP-based composites should exhibit excellent biocompatibility. Research described in this article has already yielded remineralizing sealants and orthodontic adhesives as well as a prototype root canal sealer. Our work has also contributed to a better understanding on how polymer matrix structure and filler/matrix interactions affect the critical properties of these polymeric composites and their overall performance. The addition of antimicrobial compounds to the formulation of ACP composites could increase their medical and dental regenerative treatment applications, thereby benefiting an even greater number of patients.

KEYWORDS: amorphous calcium phosphate, bioactivity, dental composite, polymerization, remineralization

*Corresponding author: drago.skrtic@nist.gov

INTRODUCTION

Calcium phosphates in dental and biomedical applications

Calcium phosphates (CaPs) are of special significance to oral biology, dentistry and medicine due to their occurrence in both normal (enamel, dentin and bone) and pathological (atheroschlerotic deposits, urinary calculi, and dental calculi) mineralization. CaPs are, generally, non-toxic, biocompatible, non-antigenic, and they integrate into living tissue by the same processes that are active during bone formation [1-5]. Within the CaP family of compounds, there are a number of crystalline forms with very distinctive structural, compositional and solubility features. Hydroxyapatite (HAP; idealized as $Ca_{10}(OH)_2(PO_4)_6$) is considered to be the final, stable product in the precipitation of CaPs from neutral and/or basic solutions. HAP is also the main mineral component of bones and teeth. Biological HAPs typically are not pure-stoichiometric but rather carbonate-substituted and calcium-deficient. Over the broad range of solution conditions in which CaPs form spontaneously, amorphous calcium phosphate (ACP; approximate compositional formula $Ca_3(PO_4)_2.3H_2O$ [6]) precedes the appearance of HAP. ACP lacks the long-range, periodic atomic scale order of crystalline materials. Although the structural uniqueness of ACP has been a subject of considerable interest, of greater relevance to understanding the dynamics of HAP formation is the instability of ACP in

aqueous environments. Significantly, the solution life of ACP can be extended by the inclusion of simple cations (Mg^{2+}, Sr^{2+}, Zn^{2+}, Zr^{4+} etc.), certain anions (fluoride, silicate, carbonate, pyrophosphate etc.), various polyelectrolytes, and bio-macromolecules such as casein phospho-peptide (CPP) [2, 3]. In aqueous environments, and particularly under acidic challenges, a spontaneous, autocatalytic ACP to HAP conversion occurs accompanied by the simultaneous release of Ca and PO_4 ions. This release of mineral constituent ions is seen as a major advantage of ACP-based biomaterials compared to the crystalline CaP-based counterparts.

Our group at the Volpe (formerly known as Paffenbarger) Research Center has been at the forefront of the research on bioactive, remineralizing polymeric ACP dental materials for over two decades. Our work was initially driven by the considerable experience of our team in ACP synthesis and its thermodynamic and solution kinetic behavior. It was further inspired by the ACP's proven biocompatibility, osteoinductivity, affinity for proteins and cells [2, 3], and its resorption rate coinciding closely with the rate of new bone formation [2]. ACP showed better osteoconductivity *in vivo* than HAP [7] and has been recognized as a precursor to HAP formation both *in vitro* and *in vivo* [4, 8-12]. It has also been identified in early formed enamel [13]. We have demonstrated that polymeric ACP composites, when exposed to simulated oral conditions, indeed provide an extended reservoir of Ca and PO_4 ions needed for the repair of damaged tooth mineral, and can efficiently regenerate mineral-depleted tooth structures *via* re-deposition of HAP [14]. Besides its practical applicative side, our work has also contributed to a better understanding of ACP/polymer and ACP composite/tooth interfacial phenomena, and the bio-responses to these types of materials. In this article, we describe the experimental designs used to formulate ACP composites for various dental applications and also explain how have our studies helped us and, possibly a much wider scientific research community, to better understand how different monomer systems yield unique matrix structures and filler/ matrix interactions that can affect many critical properties of ACP composites and their overall performance. We also discuss our future directions aimed at adding an antimicrobial function in the formulation of ACP composites, adhesives, sealants, etc., thus possibly further expanding the potential application of ACP composites not only in dentistry but perhaps in regenerative hard tissue medicine as well.

ACP as an anti-demineralizing/remineralizing tool in dental applications

Tooth demineralization (dissolution of tooth mineral into saliva) and remineralization (re-deposition of Ca and PO_4 ions back into tooth structures) are dynamic processes that strongly depend on the pH of the oral environment. If these processes are well balanced there is no mineral loss. However, when the balance between demineralization and remineralization is disrupted (local decrease in pH caused by bacterial plaque or the frequent intake of acidic foods and beverages) demineralization prevails. If uncontrolled, over time this demineralization leads to tooth erosion and, in advanced cases, decay. Therefore, inhibition of the uncontrolled demineralization is the primary target in all anti-caries therapies. It is generally achieved by fluoridation of drinking water and/or administration of fluoride (F) through tooth pastes, mouthwashes and/or high F-content gels. However, due to concerns regarding fluorosis associated with the (over)exposure to F [15], there is a need to develop new approaches for caries prevention/repair that would provide anti-demineralization/remineralization function without increasing F doses and/or its administration frequency. For any treatment to be clinically successful it is essential that a protracted supply of ions (Ca, PO_4 and/or F) needed to reform mineral structures be provided and that replacement of lost mineral occurs faster than in natural salivary mineralization. The use of solutions containing remineralizing Ca^{2+} and PO_4 ions have not been successful clinically [16], particularly in the presence of F ions. On the other hand, these relatively insoluble CaPs are not easily applied and do not localize effectively at the tooth surface. One of the ACP technologies introduced casein phosphopeptide (CPP)-ACP nanoclusters in metastable solutions. These CCP-ACP nanoclusters localize at the tooth surface and prevent caries in laboratory, animal and human *in situ* caries model studies [16-19]. Our early physicochemical testing

[20-23] and the *in vitro* remineralization study [24] have shown that ACP fillers embedded in biostable methacrylate resins release Ca and PO_4 ions in a sustained manner and maintain the desired state of supersaturation with respect to tooth enamel mineral. This feature makes ACP composites a promising anti-demineralization/ remineralization tool in not only preventing the formation of new lesions, but also in actively repairing existing incipient lesions. Furthermore, ACP composites have the advantage of concentrating Ca and PO_4 release to the site of caries attack. Functional differences between the bioactive (ion-releasing) composites and the conventional biostable dental materials as well as the potential clinical benefits from ACP composites in comparison with conventional counterparts are summarized in table 1. A wide variety of dental products could be made with only small to moderate variations in chemistry and formulation. In this review, design, characterization and evaluation of ACP remineralizing sealants, liners, orthodontic adhesives and endodontic composites are discussed in more details.

Remineralizing ACP sealants and/or base/lining materials

Much has been written regarding the potential for both caries prevention and repair through remineralization, but to this day few, if any, therapeutic materials have been made available to the practitioners. Identifying an incipient interproximal lesion radiographically or a visual white spot lesion adjacent to an existing restoration is still a “wait and see” situation where all the practitioner can do is to recommend oral hygiene measures and reassess the situation at future visits. A strong need exists for restorative, adhesive and sealant materials that can be placed either permanently or temporarily in areas where carious lesions are beginning or are likely to occur, and that will reliably protect or repair those adjacent tissues. A resin-based restorative that incorporates ACP, a proven remineralizing agent, is seen as an excellent candidate material. As either a light and/or chemically cured composite, it can be placed, using the existing techniques and instrumentation, in patients with high caries risk or when remineralization of an existing incipient lesion is desired. The composite could be placed as a provisional restoration in high caries patients until disease is brought under control or as a preventive base under more permanent materials. It could also be used as a pit and fissure sealant. In all foreseen applications, ACP composite would respond to localized change in pH caused by cariogenic bacteria by releasing high concentrations of Ca^{2+} and PO_4 ions. Besides buffering the bacterial acids, these ions would also be able to remineralize enamel already damaged by the carious conditions. The main advantage of using ACP-based material would be to supply the remineralizing ions in the localized environment of the lesion without changing the mineral saturation of the entire cavity. The therapeutic material would be applied directly to the site where it is needed the most.

Remineralizing ACP orthodontic composites

Enamel demineralization is a common occurrence in orthodontics due to plaque colonization around fixed appliances. Severe cases result in carious lesions and/or unsightly white spots in enamel under and around the periphery of bonded brackets. Orthodontic bonding systems involve at least two interfaces, the enamel/adhesive and the bracket/adhesive interface. If the orthodontist chooses to use an unfilled resin (sealant), then an additional sealant/adhesive interface is introduced. In either case, control of the bond strengths resulting from the various etchant/adhesive/bracket combinations is essential. Some cements bond chemically to enamel, but bond strengths are generally low because cements are brittle and fracture cohesively [25]. Because of their physical properties and low solubility in oral fluids resins and resin-cement hybrid materials and, to a lesser extent, dental cements are used to secure fixed orthodontic devices to tooth surfaces. Resin adhesives typically yield higher bond strengths because resins are more fracture resistant than cements. Resins, however, do not bond well in the presence of moisture, and their attachment to surfaces is primarily mechanical. Hybridized materials combine the advantages of cements and resins but also have certain disadvantages, such as clinical failure rates of up to 12% [26]. Compomers and hybrid composites, behave much like resin adhesives.

Table 1. Functional differences between the bioactive (ion-releasing) composites and biostable (non-releasing) dental materials (A) and the foreseen clinical benefits of ACP composites (B).

A	**BIOSTABLE, CONVENTIONAL RESTORATIVES** Methacrylate(s) & Initiator system → Provide polymer matrix Silanized glass or Ceramic filler → Reinforces matrix by primarily covalent bonding	**BIOACTIVE RESTORATIVES** **Glass ionomers; resin modified ionomers; compomers** Polyalkenoate or Modified Polyalkenoate → Provides polymer matrix Glass filler → Releases F Reinforces matrix crosslinking **ACP composites** Methacrylate(s) & Initiator system → Provide polymer matrix ACP filler → Releases Ca and PO_4 ions
B	**DENTAL FIELD**	**BENEFIT FROM ACP COMPOSITES**
	Restorative and preventive dentistry ⟷	Cavity prevention in xerostomic patients
	Orthodontics ⟷	Minimized demineralization under orthodontic brackets
	Endodontics ⟷	Remineralizing sealers and/or fillers

Caries inhibition, as measured by fluoride release from compomers, although higher than that from resins, is generally lower than that from glass ionomer cements [25]. Establishing an appropriate milieu for promoting the repair of carious lesions in orthodontic patients remains an important consideration. However, the selection of an optimal orthodontic material and its application requires full understanding of its chemical properties and possible physical and mechanical limitations, and as such, is a great challenge for both researchers and clinicians. Mineral growth necessary for maintaining a desired demineralization/ remineralization balance under acid and/or bacterial challenges can be secured by increasing concentrations of Ca and PO_4 ions within the lesion. Provided that satisfactory bonding to both tooth surfaces and brackets is attainable, ACP orthodontic composites would have the advantage of releasing tooth mineral constituents in a sustained manner for the entire course of treatment and will efficiently protect or restore damaged mineral in caries-prone orthodontic patients.

Remineralizing ACP endodontic materials

The majority of research in endodontics has been primarily focused on the development of materials and techniques to obturate the root canals of teeth. Recent advances in regenerative endodontics for immature teeth have defined a need for mineralizing regenerative materials such as ACP. The biological basis for the therapy has received comparatively little attention and the advancement of biologically based knowledge significant to clinical endodontics is still slow [27]. The primary objective of root canal therapy is to introduce the appropriate placement of a seal between the root canal system and the periodontium. An ideal root-end filling material should not only seal the root-end cavity hermetically, but should also be biocompatible, nontoxic, insoluble in tissue fluids, non-resorbable, dimensionally stable, capable of inducing osteogenesis and cementogenesis, easy to prepare and use, sterilizable, radio-opaque, inexpensive, and not susceptible to degradation in the presence of moisture. For many years, amalgam was accepted as the material of choice for endodontic surgery. When its toxicity was seriously questioned [28], zinc oxide eugenol cements [29] and hybrid ionomer composites were proposed as alternatives [30]. The advantages and drawbacks of glass ionomers and resin modified ionomers are discussed in [31]. Mineral trioxide aggregate, a mixture of calcium silicate, calcium aluminate, calcium oxide and silicate oxide, hailed by some researchers as an ideal endodontic material [32] also has a number of drawbacks [33-36]. An ACP endodontic sealer and/or filling material with consistent remineralizing capabilities and with minimal or no cellular/tissue toxicity concerns might yield endodontic treatments with improved success rates. Its evaluation for endodontic purposes requires adding cytotoxicity and diffusion tests to the standard physicochemical and mechanical evaluations in order to identify new material(s) suitable for testing in either animal model studies and/or clinical trials.

Antimicrobial ACP composites (preliminary data and future direction)

The vast majority of the commercial dental restoratives do not possess substantial antimicrobial (AM) properties [37] verifiable in clinical trials [38]. In order to make long-lasting, biofilm-resistant restorations, the material should be made antimicrobial. Most of the efforts undertaken to add AM functionality to dental materials have been focused on the release of various low-atomic and molecular mass AMs such as zinc, silver, fluoride and iodine ions, and antibiotics such as chlorhexidine. Generally, there are numerous unresolved issues related to the AM activities of these agents such as still unclear mechanism(s) of their actions, concerns about their toxicity against human cells, general risks related to their release, and questionable long-term efficiencies of their AM action. The AM effects of all low-molecular weight AM agents are typically short-lived. Their uncontrolled release can lead or has led to compromised mechanical properties of the materials. Moreover, if the dose or release kinetics is not properly controlled, toxicity to surrounding tissues becomes a serious drawback.

By becoming part of the polymer matrix phase of dental materials, quaternary ammonium (QA) methacrylate monomers are typically utilized to impart antibacterial activity to polymeric dental composites [37, 38]. QAs are known for their AM action against both Gram-positive and Gram-negative bacteria, but are also quite toxic [39]. Recently, approach for synthesizing liquid, resin-compatible, ionic dimethacrylates based on QA salts was patented [40] and their utilization in dental applications based on the satisfactory outcome of their *in vitro* screening was proposed [41]. However, another recent study [42] revealed that incorporation of QAs into dental resin composites above a certain limit can significantly diminish mechanical strength of the materials. In addition, saliva can dramatically decrease AM activity of QA-based restoratives due to the electrostatic interactions of QA functionalities and salivary proteins which raises additional concerns about QA utilization in dental materials. To eliminate some of the drawbacks of the QAs, we intend to incorporate furanone derivatives into ACP matrices. Furanones have been indicated as the potent inhibitors of biofilm formation [43]. Their inhibitory effects appear to be mediated through the interference with the microbial communication (quorum sensing; QS) rather than the microbial growth [44]. The expectation is that

Table 2. Specific targets of our studies.

ACP materials	Aims	Success measures
ACP fillers	Hybridization and/or surface modification De-agglomeration: Effect of small ions, polymers and mechanical milling	Enhanced stability of hybrid and modified ACPs in aqueous milieu More homogeneous particle size distribution of ACPs
Sealants and/or base/liners	Resin phase modifications: structure-composition-property studies	Improved physicochemical and mechanical properties of composites by varying monomer's structure and/or function and resin composition
Orthodontic adhesives	Interfacial coupling and polymer grafting Silanization of the filler and fine tuning of the resin	Enhanced mechanical strength and adhesiveness with uncompromised remineralization capability
Endodontic sealer and/or filler	Formulation of LC-, CC and DC urethane-based ACP composites Bio-responses to copolymers and composites	High DVC without excessive PS and/or PSS Quantitative assessment of leachability and cytotoxicity
AMRE composites	Formulation of AM resins and AMRE composites Quantification of AM activity Remineralization efficacy	Physicochemical, mechanical and biological performance Biofilm formation Mineral gain/loss upon pH cycling

furanones immobilized on the surface of the restoratives will lead to a sustained AM activity, which in combination with the remineralizing (RE) action of ACP filler will render these novel AMRE composites, a new bi-directional tool for combating tooth decay.

Specific aims of the research already completed with the purpose of creating remineralizing ACP sealants, orthodontic and/or endodontic composites as well as the research planned for the near future in order to design ACP composites with AMRE capabilities, are summarized in table 2.

METHODS

The sequential steps involved in ACP composite development are presented in fig. 1. The methods and techniques typically utilized in filler synthesis and validation, as well as the formulation and evaluation of the copolymers and composites are compiled in table 3.

ACP synthesis

Generally, ACP is precipitated in closed systems (under CO_2-free N_2 to minimize CO_2 adsorption by the precipitate) at 23 °C upon rapidly mixing equal volumes of a 80 mmol/L $Ca(NO_3)_2$ solution and a 54 mmol/L Na_2HPO_4 solution that also contained a molar fraction of 2% $Na_4P_2O_7$ (known inhibitor of HAP formation). At these conditions, the ACP forms instantaneously upon mixing the reactants. Various additives (cations, surfactants and/or polymers) can be introduced during the synthesis. The reaction pH is maintained between 8.5 and 10.5. The suspensions are filtered, the solid phase washed subsequently with ice-cold ammoniated water and acetone, freeze-dried and then lyophilized. The ACPs are used as-made (am-ACP) or are subjected to milling (m-ACP; milling significantly reduces the average particle size of ACP fillers [45]). Prior to their utilization in the composite preparation, the fillers, am- and m-ACP alike, are stored under anhydrous conditions in vacuum. This precautionary step is necessary to avoid ACP's exposure to humidity and its premature conversion to HAP.

Resin formulations

The experimental resins are typically formulated from commercially available monomers. The first step in resin formulation includes mixing of the

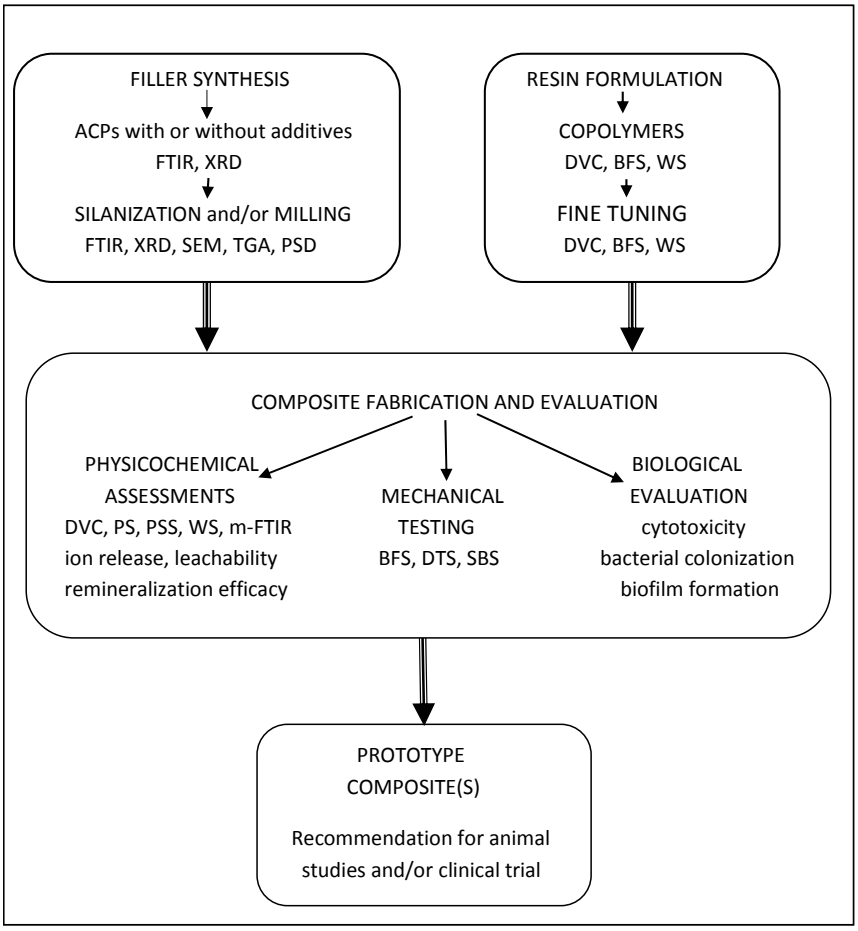

Fig. 1. Experimental steps involved in design of ACP remineralizing composites.

base monomer with diluent monomer(s). In light-cured (LC) formulations, a surface-active (adhesive) monomer(s) and the components of the visible light initiator system are sequentially added to the original mixture and the final mixture is magnetically stirred under safe lighting until fully homogenized. In chemically-cured (CC) systems, monomers are combined, homogenized and then split into two equal parts by mass. The components of the chemical-cure system are added separately to each part of the monomer mixture, and each is stirred magnetically until blended fully. In dual cure (DC) systems, LC and CC steps are combined.

Fabrication of copolymers and composites

ACP composites are made by mixing the resin (mass fraction 60%) and the filler (mass fraction 40%) by hand spatulation. Monomers and the components of polymerization initiating systems used to formulate the experimental resins are listed in table 4. To eliminate the air entrained during mixing, the homogenized pastes are kept overnight under a moderate vacuum (2.7 kPa). The LC pastes are packed into Teflon molds (mold dimensions vary depending on the type of tests to be performed), each opening of the mold is covered with a thin Mylar film and a glass slide, and the assembly clamped in place by spring clips. The specimens are photo-polymerized by irradiating sequentially each side of the mold assembly for 120 s with visible light (Triad 2000). The CC pastes are combined in 1:1 mass ratio before packing the mixture into the molds in the same manner as for the LC specimens. In DC formulations, CC specimens were additionally photo-irradiated. All specimens are stored for 24 h in air at 23 °C before being tested. LC, CC and

Table 3. Instrumental techniques used to validate ACP fillers and resins and/or determine physicochemical, mechanical and biological properties of ACP composites. Indicated acronyms are used throughout the manuscript.

Method	Property/Parameter	Application/Information
Atomic absorption spectroscopy (AAS)	Ca and co-cation contents	Chemical analysis of ACP fillers Levels of co-actions in ACP
Atomic emission spectroscopy (AES)	Ca and PO_4 concentration	Chemical analysis of ACP fillers Ion release from composites
Colorimetry	Cell viability	Cellular response to copolymer and/or composite
Contact angle goniometry	Wetting properties	Resin's hydrophilic/hydrophobic balance
Dilatometry	Polymerization shrinkage (PS)	Volume changes in composites upon curing
Fourier-transform infrared spectroscopy (FTIR) and micro-spectroscopy (FTIR-m)	Short range structure Surface composition	Structural validation of ACP fillers Degree of vinyl conversion (DVC) Intra-composite ACP to HAP conversion Surface characterization of copolymers and composites
Gravimetry	Mass changes upon aqueous immersion and/or exposure to humidity	Waters sorption (WS) and/or desorption (WD) of copolymers and composites
Laser scanning confocal microscopy (LSCM)	Bacterial surface coverage and density	AM action of copolymers and composites
Mechanical testing	Biaxial flexure strength (BFS), shear bond strength (SBS)	Mechanical performance of copolymers and composites (dry and wet)
Microradiography	Mineral content of the teeth	*In vitro* remineralization efficacy of the composites
Nuclear magnetic resonance (NMR)	Concentrations of leachable moieties	Identification/quantification of leachables from copolymers and composites
Particle size analysis	Histograms of number and volume particle size distribution (PSD)	Particle sizes (range and median diameter) of the fillers
Scanning electron microscopy (SEM)	Morphology, topology and size	Changes due to exposure of the fillers, copolymers and composites to aqueous media
Tensometry	Polymerization shrinkage stress (PSS)	Quantification of PSS in composites
Thermogravimetric analysis (TGA)	Temperature-dependent mass changes	Thermal decomposition and water content of the fillers and composites
Ultraviolet/visible (UV/VIS) spectrophotometry	Phosphate concentration	Chemical analysis of ACP fillers
X-ray diffraction (XRD)	Long-range crystalline order	Structural/compositional changes in composites

DC copolymer (unfilled resin) specimens are made by following the same procedures utilized for fabrication of the composite specimens. When the composite samples were made from commercial materials (commercial controls), manufacturer-recommended curing procedures were followed.

Atomic absorption spectroscopy (AAS), atomic emission spectroscopy (AES) and UV/VIS spectrophotometry

Ca/PO_4 ratios of ACP fillers, their Ca, co-cation and PO_4 contents are typically determined by AAS (Perkin Elmer Mo.603 spectrophotometer)

Table 4. Methacrylate monomers and polymerization-initiating components employed in the studies.

Component	Chemical nomenclature	Acronym	Mol. mass
Base monomers	2,2-bis[p-(2'-hydroxy-3'-methacryloxypropoxy) phenyl]-propane	Bis-GMA	512
	Ethoxylated bisphenol A dimethacrylate	EBPADMA	572
	Urethane dimethacrylate	UDMA	498
Diluent monomers	2-hydroxyethyl methacrylate	HEMA	130
	Di(ethyleneglycol)methyl ether methacrylate	DEGMEMA	188
	Glyceryl monomethacrylate	GMA	160
	Glyceryl dimethacrylate	GDMA	228
	Hexamethylene dimethacrylate	HMDMA	254
	2-methoxyethyl methacrylate	MEMA	144
	Triethyleneglycol dimethacrylate	TEGDMA	286
Adhesive monomers	Maleic acid	MaA	101
	Methacrylic acid	MA	86
	Methacryloyloxyethyl phthalate	MEP	278
	Mono-4-(methacryloyloxy) ethyl trimellitate	4MET	322
	Pyromellitic glycerol dimethacrylate	PMDMA	860
	Vinyl phosphonic acid	VPA	108
	Zirconyl methacrylate	ZrDMA	293
Chemical and/or photo-initiator	Butylated hydroxytoluene (stabilizer)	BHT	220
	Benzoyl peroxide	BPO	242
	Camphorquinone	CQ	166
	Ethyl-4-N,N-dimethylaminobenzoate	4EDMAB	193
	2,2-dihydroxyethyl-p-toluidine	DHEPT	195
	Bis(2,6-dimethoxybenzoyl)-2,4,4-triethylpenthyl phosphine oxide & 1-hydroxycyclohexyl phenyl ketone (mass ratio 1:1)	1850 Irgacure	264
	Phenyl-bis(2,4,6-trimethylbenzoyl) phosphine oxide	PbTMBPO	418

and/or UV/VIS spectrophotometry (Carey Model 219 spectrophotometer), after dissolving the powders in HCl solution. AAS is also utilized to determine the levels of Si incorporated during silanization of the fillers. PO_4 is determined as a blue molybdate complex in an acidified ammonium molybdate solution containing ascorbic acid and a small amount of antimony [46] at a wavelength of 882 nm. The AES (Prodigy High Dispersion inductively coupled plasma optical emission spectrometer) is used as an alternative analytical method for the chemical analysis of ACP fillers and the release of ions from the fillers and/or composites.

Thermogravimetric analysis (TGA)

Thermal decomposition profiles of ACP fillers are determined by using a Perkin Elmer 7 Series Thermal Analysis System and heating 5-10 mg of powdered ACP samples at the rate of 20 °C/min (30-600 °C temperature range) in air atmosphere. The overall water content (mass fraction, %), relative ratio of surface-bound/structural water and the level of organics (structurally-incorporated surface-modifiers) are assessed from the TGA data.

Particle size distribution (PSD)

The PSD of the ACP fillers is measured either by using a Shimadzu centrifugal particle size analyzer

(model SA-CP3) or a laser light scattering particle size analyzer (CIS-100, Ankersmid). Median particle size diameter (d_m) is taken as a primary indicator of ACP particle aggregation (the higher the d_m value, the more aggregated the ACP). The PSD data are typically compared with the results of the SEM analysis.

Scanning electron microscopy (SEM)

Surface morphology/topology of ACP powders is routinely examined by SEM using a JEOL, JSM-5400 instrument. SEM is also used to evaluate: a) composite disk surfaces before, during (disks cut perpendicular to their fiat surfaces) and after immersion in the test solutions, b) fractured surfaces of composite disk specimens resulting from mechanical testing, and c) tooth/composite interfaces before and after adhesion testing.

X-ray diffraction (XRD), Fourier transform infrared (FTIR) spectroscopy and micro-spectroscopy (FTIR-m)

The XRD profiles of powdered samples are recorded from 4° to 60° 2Θ with CuKα radiation $\lambda = 0.154$ nm using a Rigaku DMAX 2000 X-ray diffractometer operating at 40 kV and 40 mA. The samples are step-scanned in intervals of 0.010° 2Θ at a scanning speed of 1.000 deg/min. The same scanning conditions are applied to composite disk specimens that are examined for internal ACP into HAP conversion upon aqueous immersions.

The FTIR spectra [(4000-400) cm^{-1}] of the fillers are recorded using a Nicolet Magna-IR FTIR 550 spectrophotometer purged with dry air and employing the KBr pellet technique [(0.8-1.0) mg solid/400 mg KBr]. The FTIR spectra of the resins are obtained in transmission mode from thin films of the neat resins between the KBr plates.

Mid-FTIR or near-IR spectroscopy is utilized to determine the degree of vinyl conversion (DVC) of the unfilled resins (copolymers) and their ACP composites. Mid-FTIR measurements include monitoring the reduction in the 1637 cm^{-1} absorption band for the vinyl group against that of an unchanged aromatic peak (1538 cm^{-1}) used as an internal standard. Near-IR method monitors the reduction in the $=CH_2$ absorption band at 6165 cm^{-1} in the overtone region. By measuring the thickness of monomers/polymer specimens, the need to use an invariant absorption band as an internal standard is circumvented in near-IR measurements. For both methods, spectra are typically acquired before photo-cure, immediately after cure, as well as 24 h and 7 d post-cure.

The FTIR-m is employed to assess the distribution of ACP filler in the resin matrix (intact surfaces as well as cross-sectioned surfaces of copolymer and composite samples) prior (dry specimens) and after exposure to test solutions (wet specimens). A Nic-Plan IR microscope (in reflectance mode) interfaced with a Nicolet Magna-IR TM 550 FTIR spectrophotometer and equipped with a video camera to display images, a liquid nitrogen cooled-mercury cadmium telluride detector (Nicolet Instrumentations Inc.) and a computerized motorized mapping stage, programmable in the x and y directions is used for that purpose. The usefulness of FTIR-m in addressing the problems associated with filler agglomeration and in producing functional PO_4 and >C=O group maps is extensively elaborated in [47].

Dissolution/transformation (ion release) kinetics

Both powdered fillers and composite disk specimens are evaluated for their dissolution behavior at 37 °C in aqueous environment (HEPES-buffered (pH = 7.40) 240 mOsm/kg saline solutions). The kinetics of ion release is followed upon dispersion of approx. 800 mg of powdered solids or suspension of the individual composite disks (by means of a stainless steel wire frame) in continuously stirred 100 mL saline. Aliquots for Ca and PO_4 analysis (UV/VIS spectrophotometry and/or AES) are taken at the predetermined time intervals. At the same time intervals, a fraction of the solids is separated from the suspending medium, freeze-dried (necessary for early time intervals) and analyzed by XRD and FTIR to assess the extent of ACP to HAP conversion. Composite specimens are additionally screened by SEM and FTIR-m, then ground and the resultant powders analyzed by XRD and FTIR.

Remineralization potential

The remineralization potential of the fillers and composites is calculated from the maximum calcium and phosphate ion activities reached upon aqueous immersion. The thermodynamic stability

of these solutions is calculated with respect to the stoichiometric HAP using the Gibbs free-energy expression:

$\Delta G° = - 2.303(RT/n)\ln(IAP_{HAP}/K_{sp})$

where IAP_{HAP} is the ion activity product for HAP defined as $IAP_{HAP} = \{Ca\}^{10}\{PO_4\}^{6}\{OH\}^{2}$, K_{sp} is the corresponding thermodynamic solubility product, R is the ideal gas constant, T is the absolute temperature, and n is the number of ions in the IAP (n = 18). Negative $\Delta G°$ values indicate solution supersaturation with respect to stoichiometric HAP (K_{sp} = 117.2) and are taken as a measure of remineralization ability.

Mechanical properties

Biaxial flexure strength (BFS) and shear bond strength (SBS) of copolymers and experimental composites are determined by using a computer-controlled Universal Testing Machine operated by Testworks 4 software.

A piston-on-three-ball loading arrangement [48], suitable for even slightly warped specimen is used for the BFS measurements (pastes are pressed into a teflon mold [(15.8-16.8) mm in diameter and (1.5-2.1) mm in thickness] by using a plastic spatula). Each opening of the mold is covered with a thin mylar film and a glass slide and the assembly clamped together with a spring clip. The disks are photopolymerized by irradiating each face of the mold assembly for 2 min with visible light. After photo-curing, specimens are released from their molds and kept in either air (dry samples) or in test solutions at 37 °C (wet samples) for the duration of the immersion experiments. The BFS is calculated according to the following equation [49]:

$BFS = AL/t^2$

where $A = -[3/4\pi(X-Y)]$, $X = (1+v)\ln(r_1/r_s)^2 + [(1-v)/2](r_1/r_s)^2$, $Y = (1+v)[1 + In(r_{sc}/r_s)^2]$, and where v = Poisson's ratio, r_1 = radius of the piston applying the load at the surface of contact, r_{sc} = radius of the support circle, r_s = radius of disk specimen, L = applied load at failure, and t = thickness of disk specimen.

The SBS tests are performed on extracted human teeth embedded with cold-cured resin in poly-carbonate cups. Exposed dentin surfaces of the tooth samples will be ground fiat at a 90° angle to the longitudinal axis of the polycarbonate holder. Photo-activated pyromellitic glycerol dimethacrylate (PMGDMA) in acetone solution is used to establish an adhesive layer between the exposed dentin and composite. A brass ring (4 mm in diameter and 1.5 mm in thickness) is used as a mold for the composite. Teflon tape (0.3 mm thick) with a hole coinciding with the hole in the ring will be placed under the brass ring to prevent the ring from adhering to the dentin. Both the ring and the tape are placed in the center of the dentin surface and held down with a lead weight (450 g). The cavity in the brass ring is filled with the composite, irradiated for 1 min with a commercial visible-light source, and stored (at 37 °C) immersed in distilled water for various time intervals before de-bonding. To determine the SBS, The assembly is placed against the vertical surface of a nylon block. The ring-enclosed composite is sheared off at a cross-head speed of 0.5 mm/min with a flat chisel pressing against the edge of the brass ring and connected to the load cell of the testing machine. The analysis of fractured specimens is performed by digitally photographing (Leica MZ16 Optical Stereomicroscope) tooth and iris, and measuring the surface areas of different failure modes (Image J, NIH).

Water sorption (WS)

WS tests are typically performed with the broken disk specimens collected after mechanical testing of dry samples. To determine WS of copolymer and/or composite specimens, a minimum of 7 disks/experimental group are initially dried over $CaSO_4$ until a constant mass (± 0.1 mg). Specimens are then immersed in saline solutions as described for ion release experiments. Gravimetric mass changes of padded dry specimens are recorded at predetermined time intervals. The degree of WS is calculated using a simple equation:

$WS = [(W_t-W_o)/W_o] \times 100$

where W_t represents the sample mass at the time t, and W_o is the initial mass of dry sample.

WS data are used to calculate the diffusion coefficient (D) by applying the simplified Fick's model (valid for the sorption stages when $W_t/W_{eq} \leq 0.6$):

$W_t/W_{eq} = (2/L)x(Dt/\pi)^{1/2}$

where W_t is the mass gain at time t, W_{eq} is the mass gain at the equilibrium, and L is the thickness of the specimen. D is calculated from the slope of the plot of W_t/W_{eq} vs. $t^{1/2}$.

In some systems, WS is determined by exposing dry specimens to an air atmosphere of 75% relative humidity (RH) at 23 °C (specimens are suspended over saturated NaCl slurry in closed systems) and recording gravimetric changes in the same manner as with saline-immersed specimens. WS data collected at 75% RH are unaffected by dissolution of ACP filler or leaching of water-soluble monomers and/or polymer degradation products (in saline-immersed specimens, these processes typically occur in parallel to WS).

Polymerization shrinkage (PS)

The PS of composite resin samples is measured by a computer-controlled mercury dilatometer developed at the VRC-ADAF. Composite pastes are cured using a standard 60 s/30 s exposure and data acquisition of 60 min + 30 min. The PS of a specimen corrected for temperature fluctuations is plotted as a function of time. The overall shrinkage (volume fraction, %) is calculated based on the known mass of the sample (50 mg-100 mg) and its density. The density is determined by means of the Archimedean displacement principle using an attachment to a microbalance.

Polymerization shrinkage stress (PSS)

The tensometer, designed and fabricated at the VRC-ADAF, is utilized to assess the PSS [50] of the experimental composites. The corresponding software program has also been developed at VRC-ADAF. The design of the sample assembly facilitates convenient sample injection, experimental reproducibility and a short preparation time between the consecutive measurements. The PSS is obtained by dividing the measured tensile force by the cross sectional area of the sample.

Quantitative microradiography

The microradiographic remineralization studies are performed with artificially created caries-like lesions in human and/or bovine enamel. Details on teeth collection, storage, creation of subsurface lesions by immersion in demineralizing solutions (DeS) and the preparation of tooth sections are detailed in [24, 51-53]. Contact microradiographs are produced by exposing the individual tooth specimens to CuKα radiation (40 kV, 3 mA) and developing films according to manufacturer's recommendations. Mineral density is established relative to sound enamel for each sample. After the initial contact microradiographs are taken, the individual tooth sections are assembled between parafilm and glass cover slips in the following order: cover slip/parafilm/tooth slice/parafilm/cover slip. The demineralized edge of the tooth slice is kept even with one side of the assembly and left exposed while the rest of the assembly is wrapped and embedded in strips of parafilm to seal around the edges. It is then sandwiched between two glass slides, with the exposed edge of the tooth section positioned approximately 1 mm below the slide edges. The demineralized surface is coated with a (1.0 ± 0.1) mm thick layer of the experimental composite, HAP-containing composite and/or the commercial control, or left untreated. Composites are light-cured for 60 s (Triad 2000). After photo-curing, the individual assemblies of composite specimens and/or uncoated controls that required no curing are subjected to pH-cycling regimens which mimic demineralization and remineralization cycles occurring daily in the oral environment. The assembled tooth specimens are alternately immersed at 37 °C, under continuous magnetic stirring (38 rad/s), in DeS (0.5 h) and remineralizing solution (ReS; 11.5 h) for 14 days (bovine teeth series [24]), or in DeS (1 h) and ReS (23 h) for 30 days (human teeth series [51]). At every solution exchange, the assemblies are thoroughly rinsed with distilled water. Mineral profiles of each specimen before and after the completion of the pH cycling regimen [52, 53] are determined by digital-image-analysis of the corresponding contact microradiographs using the commercial system Bioquant IV interfaced with an optical microscope (Leitz) for bovine teeth and Scion Image-release Alpha 4.0.3.2 (NIH) interfaced with an optical microscope (Olympus BX50F) and digital camera (RGB/YC/NTSC; Microimage) for human teeth. Changes in lesion depth and mineral loss (ΔZ) are compared for each imaged area before and after treatment. The difference in summed ΔZ values across the depth of each lesion before and after the pH-cycling regimen, i.e., the

relative change in mineral content, $\Delta(\Delta Z)$ in %, is calculated according to the following equation:

$$\Delta(\Delta Z) = \{(\Delta Z_{before} - \Delta Z_{after})/\Delta Z_{before}\} \times 100$$

The mean $\Delta(\Delta Z)$ values obtained for all image areas of each group of specimens were used to indicate remineralization (positive (+) $\Delta(\Delta Z)$ values) or further demineralization of the lesions (negative (–) $\Delta(\Delta Z)$ values) as a result of pH-cycling treatment.

Leachability studies: ^{1}H-Nuclear magnetic resonance (^{1}H-NMR) spectroscopy

Following the extraction of copolymer and composite disk specimens in a series of organic solvents and measuring their total weight loss, the residual solvent-free extracts are analyzed in $CDCl_3$ by ^{1}H-NMR (GSX 270, JEOL). The NMR calibration curves are calculated relative to BHT which is utilized as an inhibitor of monomer polymerization upon extraction. BHT's shift serves as an internal standard. Detailed description of the methodology and NMR data interpretation is provided in [54].

Micro-leakage (dye penetration)

The appraisal of the sealing efficacy of endodontic materials is not included in the international standards covering root canal sealers. In the absence of standardized test protocol, a number of different *in vitro* methods are being used for that purpose. We assess the micro-leakage of ACP endodontic sealants by a dye penetration method. For that purpose, root canals of the extracted teeth are prepared as described in [55] and filled with Resilon™ (a synthetic polymer-based root canal filler) and sealed with the experimental ACP sealer (experimental group) or filled with Resilon™ sealed with commercial resin sealer EndoREZ™ (control group). EndoREZ™ is chosen due to the fact that its main resin component is UDMA-based, similar to the experimental ACP material. After curing, specimens are stored in saline solutions at 37 °C for 72 hours to allow sufficient time for the completion of the setting process. The root surfaces, except for the apical 2 mm (in this way dye could penetrate the canal only *via* apical region) are then covered with two layers of nail varnish and specimens placed into 2% methylene blue dye solution for a week at 37 °C. After removal from the dye solution, washing with distilled water and drying, teeth are sectioned longitudinally in a bucco-lingual direction through the center of the root. Linear apical leakage is estimated using a stereomicroscope (Leica MZ16, Wetzlar, Germany).

Cell responses to copolymers and ACP composites

To assess the cellular responses to experimental copolymers and their corresponding ACP composites, specimens are typically extracted in media overnight and then the osteoblast-like cells (MC3T3-E1 cells; Riken Cell Bank) are cultured in these extracts [56]. Cytotoxicity is evaluated by phase contrast microscopy and an enzymatic assay is used for mitochondrial dehydrogenase activity (Wst-1).

Prior to extraction experiments, all disk specimens are sterilized with 70% ethanol. Each disk is then washed with 2 mL of media for 1 h and then fresh media was placed on each disk for an overnight extraction in the cell incubator. Positive (containing media with surfactant) and negative (containing only media) controls are evaluated in addition to composite and copolymer specimens. In parallel, a flask of 80% confluent MC3T3-E1 cells were passaged, cells seeded into well plates with 10,000 cells per well in 2 mL of media, and then placed in the incubator overnight. On the second day of the experiment, the medium from each "cell well" is removed and replaced with the 2 mL of extraction medium from one of the disk specimens (or with the positive or negative control media). The cells are incubated in the extracts for 3 d, photographed and then prepared for the cytotoxicity assays.

The Wst-1 colorimetric assays are performed as follows: extract-cultured cells and the controls without cells are combined with a Wst-1 solution (2-(4-iodophenyl)-3-(4-nitophenyl)-5-(2, 4-disulfophenyl)-2H-tetrazolium, monosodium salt) in HEPES buffer, individually added to wells and incubated for 2 h at 37 °C. Aliquots from each well are transferred to a well-plate and absorbance is read at 450 n with a plate-reader.

AM activity of copolymers and AMRE composites

To quantify the AM activities of the experimental AM resins and their corresponding AMRE

composites, the initial bacterial colonization and suppression of biofilm formation are assessed in the following manner. Copolymer and composite disk specimens are first sterilized with ethanol (70 mass %) for 20 min and then soaked in phosphate buffered saline overnight. To assess the initial bacterial colonization, specimens are inoculated with *Streptococcus mutans* (*S.m.*), and then incubated (37 °C, 5 vol. % CO_2) for 5 h. Following the incubation, samples are triple-washed to remove non-adherent bacteria, fixed with formaldehyde solution, stained with SYTOX green and imaged using a laser scanning confocal microscope (LSCM). Images are quantified in terms of the total surface area covered by bacteria and the object density and plotted as a function of the concentration of AM component in the resin. To evaluate the ability of the resins and composites to suppress biofilm formation, specimens are inoculated with *S.m.* in sucrose containing (1 mass %) bovine-heart infusion and incubated for 24 h, 14 days and 1 month. In 14 days and 1 month experiments, broth is replenished daily. The same fixation, staining and the LSCM imaging protocols, and data interpretation are used as for the initial *S.m.* colonization tests.

Statistical methodology

The number of test specimen for each evaluation step is chosen so that there is a reasonable chance (power) to detect the minimum desired difference between the groups [57]. The variance estimates used in the calculation are obtained from historical data (e.g. previous work or literature). Graphical data analysis, analysis of variance (ANOVA), and other related tests [58, 59] are performed to evaluate the experimental data as a function of composite makeup, storage times or any other relevant factor involved in the experimental design. For those cases where overall statistically significant effects are found with ANOVA, further tests are performed to determine the significant differences between the specific groups using an appropriate multiple comparison procedure. All tests are 2-sided at $\alpha = 0.05$. Statistical analyses of the data are done by means of Microsoft Excel or NIST Dataplot^{TM}, SYSTAT9 or SigmaStat (version 2.03). Throughout this review, one standard deviation (SD) is routinely indicated as the estimated uncertainty of the measurements.

RESULTS AND DISCUSSION

The long-term, ion-releasing characteristics of ACP-based polymeric materials make them especially advantageous in dental applications designed to prevent demineralization and/or promote remineralization. However, bioactive ACP composites are generally relatively weak because ACP does not act as reinforcing filler in a manner similar to that of commonly used silanized glass fillers. The uncontrolled aggregation of ACP during its spontaneous precipitation typically leads to heterogeneous distribution of the filler in the resin, thus hindering the interfacial resin-filler interactions and compromising the mechanical performance. The uneven distribution of highly aggregated filler in composites may also affect the ion release from these materials. To address these shortcomings, surface-modification of ACP fillers and their mechanical milling were explored as described below.

Effects of additives on physicochemical characteristics of ACP fillers and Bis-GMA/TEGDMA composites

The hypothesis was that interactions between the ACP and additives (small ions and surfactant or polymer molecules) would affect the extent of ACP particle aggregation and its stability in aqueous environments. The mechanism and the extent of additive/ACP interaction should primarily depend on the chemical nature of additives. Cation-ACP interactions are expected to be controlled by the ionic potential, i.e., the water coordination number, multiplicity of charge and ionic radius [60]. In the case of polyelectrolytes, the multiplicity of the ionizable groups is expected to be a major regulatory factor. Generally, hybridization of ACP fillers is expected to yield bulk-modified ACPs with greater potential for strengthening the composites without compromising their remineralization potential. To test the above hypotheses, additives were introduced *ab initio*, the amorphous nature of the resulting solids validated by FTIR, XRD, and the effects of additives on PSD, water content and remineralization potential were assessed. In addition,

the BFS and DVC of the composites formulated with Bis-GMA/TEGDMA resin and surface-modified ACPs were determined. The results are summarized in fig. 2 A, B. Introducing cations, surfactants and polymers during the spontaneous precipitation of ACP from supersaturated Ca and PO_4 solutions marginally reduced or had no significant effect on the overall water content of

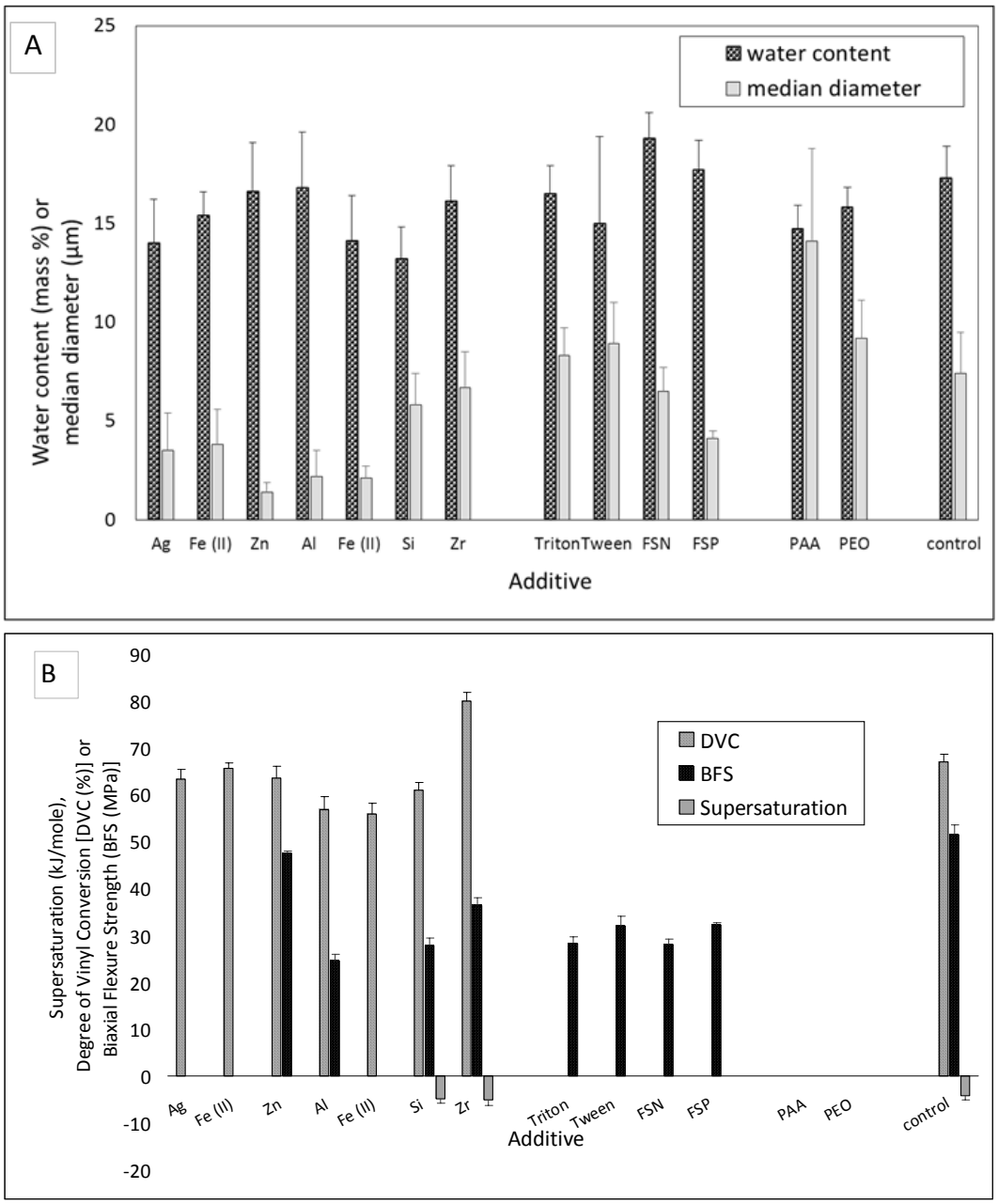

Fig. 2. Water content (TGA data) and particle size (PSD data; median diameter - d_m) of surface-modified ACP fillers (**part A**). DVC, BFS and remineralization potential [expressed as supersaturation of the immersing solutions [Gibbs free energy, ΔG^o]] attained in light-cure Bis-GMA/TEGDMA composites formulated with various ACPs (**part B**). Number of runs: $n \geq 5$ for DVC and BFS measurements, and $n \geq 3$ for PSD, TGA and ΔG^o assessments. Indicated are mean values with one standard deviation (SD).

the isolated solids (on average 15.3, 14.8 and 17.1 mass % for cation-, polymer and surfactant-ACPs, respectively, compared to 17.3 mass % for no-additive control). Additives also did not alter the ratio of surface-bound/structurally incorporated water in ACPs; the average ratio of 2.4 suggests that approx. 70% of water in ACPs is labile and the remaining 30% is structurally incorporated. In cation series, the mean particle diameter, d_m, decreased in the following order: (Si-, Zr-ACP) > [(Ag-, Fe(II)-, Al-, Fe(III)-ACP) ≥ Zn-ACP]. This decrease in d_m was accompanied with the reduction in the PSD range (from up to 80 μm in Si- and Zr-ACP to only 15 μm in other cation ACPs). The unwanted color change occurred in Ag- and both Fe-ACPs. It was due to the co-precipitation of light-sensitive Ag-phosphate and colored Fe-phosphates in parallel to ACPs. In addition, Fe-ACPs showed signs of premature ACP to HAP conversion. The PSD of surfactant-modified ACPs did not significantly change compared to no-additive control except for the anionic fluorosurfactant (FSP), where a 45% reduction in d_m was seen. In polymer group, instead of particle size reduction, a 25% and a 90% increases in d_m were observed, respectively, with PAA and PEO (irrespective of the PEO molecular mass). The experimental composites formulated with cation-ACPs (Ag^+, Fe^{2+}, Zn^{2+}, Al^{3+}, Fe^{3+} and Si^{4+}), surfactant-ACPs and polymer-ACPs generally exhibited inferior mechanical stability compared to the control ACP. The reduction in BFS varied from 33-45% for surfactant- and polymer-ACPs and 6-100% for cation-ACPs (Ag- and Fe-ACPs disintegrated upon immersion). Only Si- and Zr-ACP based composites showed improvements in DVC (9% and 19%, respectively). Zr-ACP based composites also performed better than control with respect to remineralization potential (22% increase) and BFS (27% increase). For those reasons, Zr-ACP was chosen as "gold standard" filler and was used for all subsequent studies described in this review.

Effect of mechanical milling on PSD of the fillers and remineralization potential of the composites

Ball milling (experimental details are provided in [61]) of Zr-ACP filler prior to its utilization in composites is evaluated as an alternative way of reducing the average size of ACP by breaking up large aggregates into smaller agglomerates that will more intimately interact with the resin and disperse more evenly in the composite. The experimental composites were formulated from LC EBPADMA/TEGDMA/HEMA (ETH) resins and the unmilled and milled ACP fillers. The composites were assessed for their mechanical behavior and the kinetics of mineral ion release. Such an assessment is deemed necessary in order to ensure that improvement in mechanical strength of composite is achieved without compromising the remineralizing ability of composites. The results are summarized in table 5.

While having no apparent effect on the structure (amorphous character retained after milling) and composition (Ca/PO_4 ratio and water content of the solids remained unchanged), milling

Table 5. PSD data (n = 3/group) comparison for the as-made and milled Zr-ACP fillers. The mechanical strength (BFS; n ≥ 3) and the remineralizing potential (ΔG^o; n = 3) of the ensuing ETH composites. Indicated are mean values with one standard deviation (SD) given in parenthesis.

Parameter	Zr-ACP filler (as-made)	Zr-ACP filler (milled)
Median diameter, d_m (μm)	5.93 (0.69)	0.90 (0.19)
PSD range (μm)	0.3-80.0	0.2-3.0
Specific surface area (m^2/g)	0.49 (0.10)	3.80 (0.10)
	as-made Zr-ACP ETH composite	**milled Zr-ACP ETH composite**
Ionic activity product, IAP	99.3 (0.7)	101.2 (1.0)
ΔG^o (kJ/mole)	5.7 (0.2)	5.1 (0.3)
BFS (MPa)	49 (8)	61 (8)

significantly reduced the average size of ACP particulates and the spread of their PSD. Better dispersion of milled Zr-ACP in the resins resulted in the improved BFS of the composites after aqueous immersion. The differences in the BFS values of the ETH composites made with the as-made (coarse) ACP and milled (fine) ACP may possibly be explained by the different degrees of water penetration at the ACP/resin interfaces. Thus, an accelerated diffusion and enhanced hydration most likely occurred in composites made with as-made ACP while these same processes were inhibited or reduced in composites with milled ACP. Milled-ACP composites also maintained satisfactory ion release. The maximum concentrations of Ca and PO_4 ions released from milled ACP-containing disks into immersing solutions remained highly supersaturated with respect to HAP, thus preserving a significant remineralization potential of these composites.

ACP sealants and/or base/liners

Initially, bioactive composites formulated as a remineralizing sealant and base/liner comprised hybrid Zr-ACP and a polymer blend of Bis-GMA/TEGDMA, plus HEMA and/or ZrDMA (BT, BTH and BTHZ resins; [20-23]). However, the mechanical strength of these composites, even after silanization of the filler, remained inferior to that of the conventional, bioinert, silanized glass-filled dental composites, thus diminishing the clinical appeal of these ACP materials. To possibly make ACP composites more clinically attractive, we included various surface-active monomers (X) with potentially stronger affinity for ACP into ternary Bis-GMA/TEGDMA/X blends and assessed their effects on DVC and BFS of the ensuing ACP/BTX composites. Differently structured neutral and/or acidic monomers with varying hydrophilicity included hydroxyl- and/or carboxylic acid-containing monomers (Table 6). They were expected to interact favorably with ACP *via* hydrogen-bonding and ion-binding. Besides possibly enhancing the mechanical performance of the composites, inclusion of X in the resins was also expected to yield composites with the uncompromised DVC.

Table 6. Composition (mass %) of experimental BTX resins. X = DEGMEMA, GDMA, GMA, HEMA, MEMA and photoinitiator system = CQ (0.2 mass %) and 4EDMAB (0.8 mass %) in neutral termonomer series. X = MA, MaA, 4MET, VPA and photoinitiator = PbTMBPO (2.0 mass %) in acidic termonomer series. The termonomer (X) was introduced at mass level corresponding to an equivalent molar mas of HEMA (neutral termonomer series) or 4MET (acidic termonomer series). HEMA level in BTH resin corresponded to the concentration yielding the most favorable ion release properties [22]. The level of 4MET in BT4M formulation was determined by its solubility in BH resin.

Resin/ monomer	Bis-GMA	TEGDMA	HEMA	MEMA	DEGMEMA	GMA	GDMA	VPA	MA	MaA	4MET
BTn	49.5	49.5									
BTH	37.0	37.0	25.0								
BTM	35.7	35.7		27.6							
BTD	31.5	31.5			36.0						
BTGm	34.0	34.0				31.0					
BTGd	27.0	27.0					45.0				
BTa	49.0	49.0									
BTV	48.2	48.2						1.6			
BTMA	48.4	48.4							1.2		
BTMaA	48.2	48.2								1.6	
BT4M	46.6	46.6									4.8

The results of the BFS testing (after immersion in saline) and DVC screening (24 h-post LC) for both BTX series are presented in fig. 3. In BT/neutral termonomer series, the mean BFS value of the BTn control [(52.3 ± 5.1) MPa] significantly exceeded the BFS values of all formulations [on average (29.9 ± 7.9) MPa]. Disruption by water of the hydrogen bond-mediated crosslinks may explain this precipitous drop in BFS values. In BT/acidic termonomer series, the BFS values decreased in the following order: BT4M [(66.5 ± 13.3) MPa] > BTa control [(48.4 ± 6.7) MPa] > BTMA, BTV and BTMaA [average (32.0 ± 4.2) MPa]. Generally, the reduced mechanical strength in acidic BTXs series is caused by reduction in ACP's intactness and rigidity at the filler/matrix interface due to the chemical reactions involving carboxylic groups and ACP, special changes that may have occurred during Ca and/or PO_4 ion efflux, internal ACP to HAP conversion and excessive water sorption. It is, however, significant that 4MET comonomer yielded composites with improved mechanical strength. DVC data analysis indicated the following order in neutral termonomer series: BTD [(75.3 ± 3.3) %] > BTH, BTn and BTGm [(67.5 ± 1.5) %] > BTM and BTGd [(61.3 ± 3.3) %]. The DVC of composites in BT/acidic series showed practically no dependence on structural variations of the acidic comonomer [average DVC = (66.0 ± 3.0) %]. The monomer system based on DEGMEMA, i.e., the BTD resin, showed the highest DVC probably because of the highly flexible nature of this monomer. As a result of this study, it would seem that the inclusion of DEGMEMA and 4MET, at optimum levels into the polymer matrices may aid in attaining a higher level of DVC while maintaining the mechanical integrity of composites upon aqueous immersion.

ACP orthodontic composites

Fine tuning of the resin composition was utilized to tailor remineralizing ACP EBPADMA-based composites for orthodontic applications. In our earlier work [14], EBPADMA, TEGDMA and HEMA were identified as a base monomer, a diluent monomer and a surface-active monomer, respectively, in polymers yielding high levels of DVC. High DVC would imply low leachability of unreacted monomeric species, thus making the composites more biocompatible. Hydrophilic TEGDMA and HEMA monomers at high levels, however, may adversely affect the mechanical properties of composites due to the excessive WS

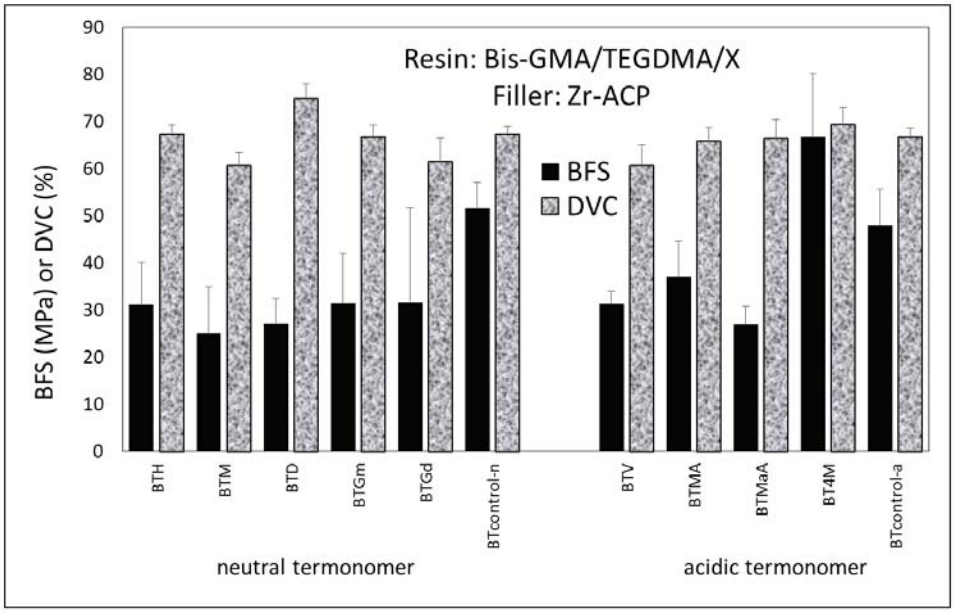

Fig. 3. Bis-GMA/TEGDMA/X (X = neutral or acidic termonomer) composites. Post-immersion BFS (n ≥ 5) and DVC 24 h post LC (n ≥ 6). Indicated are mean values + SD.

upon aqueous exposure. For these reasons, chemistry and composition of the LC EBPADMA/TEGDMA/HEMA resin (photoinitiator: IRGACURE 1850 at 1 mass %) were tuned by changing the EBPADMA/TEGDMA ratio (mass ratio 1.00, 0.67, 0.50 and 0.25 corresponding to molar ratios of 0.500, 0.333, 0.250 and 0.125, respectively) and lowering the content of HEMA to 10 mass % while including less hydrophilic carboxylic acid monomer MEP at 5 mass %. The ensuing resins were annotated ETHM100, ETHM067, ETHM050 and ETHM025. The inclusion of MEP was expected to enhance the adhesion of composite to tooth surfaces due to its known surface activity. In addition, MEP was also expected to provide more adhesive interphase *via* carboxylate-ACP interactions that would promote ACP/resin coherence. Additionally, WS and PS were expected to be reduced without a detrimental effect on the remineralizing potential and/or mechanical strength of the composites. The results are presented in fig. 4 (BFS and DVC) and fig. 5 (WS, PS and remineralization potential). Generally, the BFS [overall value (47 ± 7) MPa], DVC [overall value (84.0 ± 5.2) %], WS [overall value (3.45 ± 0.50) %] and the remineralizing capacity [overall ΔG^o = - (4.66 ± 0.31) kJ/mole] of ETHM composites showed no correlation with the resin matrix composition. However, the PS increased with decreasing EBPADMA/TEGDMA ratio in the resin. In comparison with the typical Bis-GMA based polymers, those based on a more hydrophobic analog of Bis-GMA, i.e., EBPADMA should, generally, exhibit higher DVC and lower PS. Regardless of the EBPADMA/TEGDMA ratio in the resin, the ETHM composites attained significantly higher DVCs compared to Bis-GMA-based BTX composites [84.0% vs. (61.3 to 75.3) %, respectively]. This increase in DVC values is primarily attributed to the bulkier yet flexible structure and lower viscosity of EBPADMA compared to Bis-GMA resin systems.

The PS of ETHM composites was apparently controlled by the relative content of the high molecular mass EBPADMA in the polymer matrix. Although highly desirable in order to render resin matrices less susceptible to the softening effects of the oral media and keep unwanted leachables at minimum, high DVC also resulted in higher PS. The reduction in the PS of ETHM composites, based on the inclusion of higher levels of EBPADMA relative to TEGDMA may be necessary to make them more appealing for orthodontic applications. The mechanical strength (i.e. BFS) and the WS of ETHM composites were unaffected by the composition of the resin. The average WS of

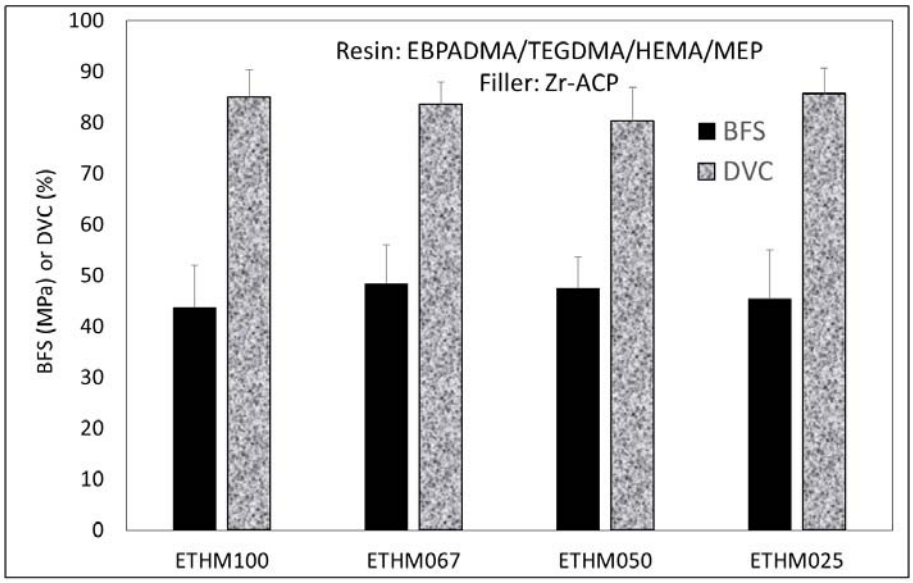

Fig. 4. EBPADMA/TEGDMA/HEMA/MEP composites. BFS after 40 days of immersion in buffered saline (n ≥ 5) and DVC 24 h post LC (n ≥ 6). Indicated are mean values + SD.

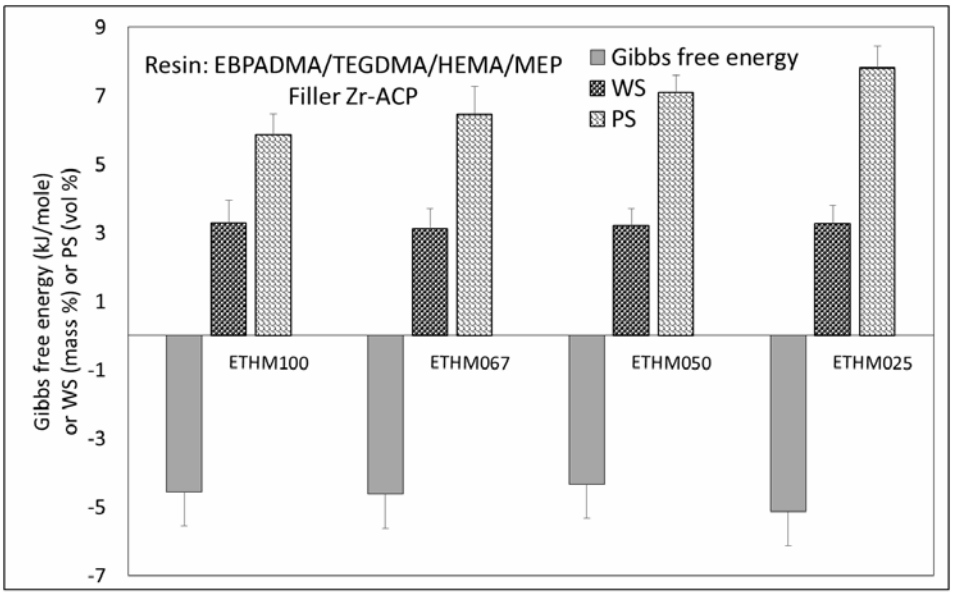

Fig. 5. The thermodynamic stability of the solutions containing maximum concentrations of Ca and PO_4 ions released from EBPADMA/TEGDMA/HEMA/MEP (ETHM) composites (Gibbs free energy indicates relative supersaturation with respect to stoichiometric HAP ($n \geq 4$)), PS ($n \geq 3$) and the maximum WS values (after 42 d exposure to 75% RH at room temperature; $n \geq 5$) of ETHM composites. Indicated are mean values + SD.

ACP/ETHM composites falls within the range reported for commercially available bonding resins (< 4 mass % [62]). It seems that the uneven dispersion of large ACP aggregates within the ETHM polymers controlled the overall mechanical performance of composites. Better control of both the PSD and surface properties of the ACP filler may be required to enhance ACP/ETHM matrix interactions and make these composites amenable as orthodontic adhesives. Generally, the enhanced ion release from composites formulated with EBPADMA and HEMA in their polymer phase is attributed to the tendency of EBPADMA to form less densely cross-linked polymeric networks and the potential of HEMA to promote mineral saturation *via* increased water uptake. In ETHM composite series, a moderate reduction in remineralizing ability compared to non-MEP containing ETH composites [ΔG^o_{ETHM} = - 4.66 kJ/mole vs. ΔG^o_{ETH} = - 5.07 kJ/mole] was due to the inclusion of 5 mass % MEP into the resin. Overall ion release, although significantly above the theoretical minimum necessary for remineralization, diminished because of the lower levels of free calcium in the solution. This reduction in solution calcium levels was caused by concomitant calcium binding by the carboxylic functionalities of MEP.

ACP endodontic materials

The working hypothesis was that resins (designated UPHM) comprising UDMA (47.2 mass %), PEG-U (29.1 mass %), HEMA (16.7 mass %) and MEP (2.9 mass %), and their ACP composites would attain high DVCs without excessive PS and/or PSS while maintaining desirable remineralization potential. In addition, the anticipated relatively high WS of ACP/UPHM composites was expected to be accompanied by their significant hygroscopic expansion (HE) upon aqueous immersion. It was also expected that the relatively high WS will not diminish the mechanical strength of composites more than it is customarily seen in other types of ACP methacrylate composites. To test these hypotheses, DC UPHM copolymers and composites were formulated with as-made and milled Zr-ACP (40 mass %) and tested for DVC, BFS, WS, HE, PS and PSS. DC systems [LC: Irgacure 1850 (1.0 mass %); CC: BPO (2.0 mass %) + DHEPT (1 mass %] were investigated since, due to the nature of the intended application, LC alone was considered as clinically inadequate. Sr-glass/UPHM composites

(70 mass % filler) were used as a control. The results are summarized in figs. 6-8. DC ACP UPHM composites, generally, attained high DVC [overall value (81.7 ± 2.4) %] and a moderate to low BFS values [overall (45 ± 7) MPa]. Both DVC and BFS of composites formulated for endodontic uses paralleled the values obtained with the ACP ETHM composites intended for orthodontic application. The high DVCs attained in ACP UPHM composites, similarly to ACP ETHM formulations intended for orthodontic utility, again suggest a minimal possibility for leachability of unreacted monomers and/or components of the initiator systems, and,

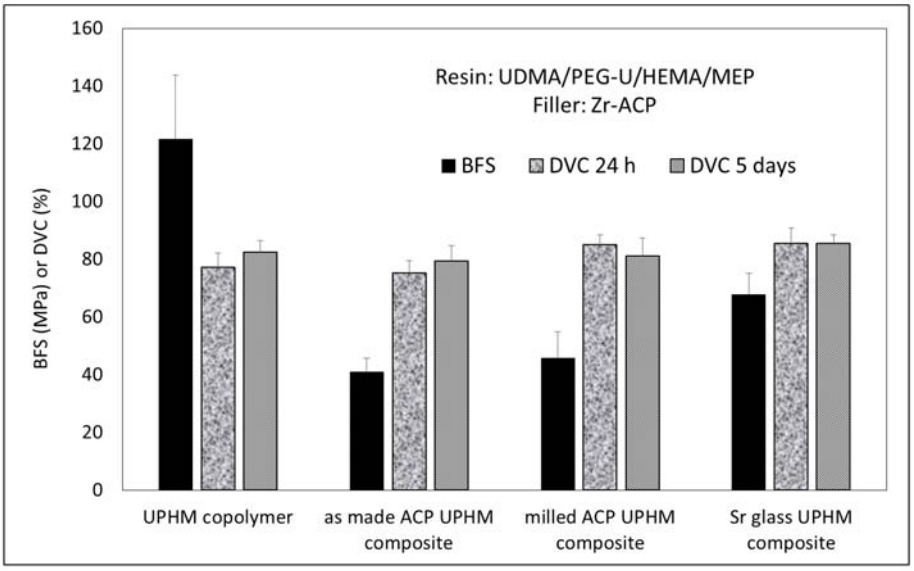

Fig. 6. BFS (after 3 months of immersion in buffered saline) and DVC (24 h and 5 days post-cure) of UDMA/PEG-U/HEMA/MEP (UPHM) copolymers and composites. Indicated are mean values + SD (n = 5).

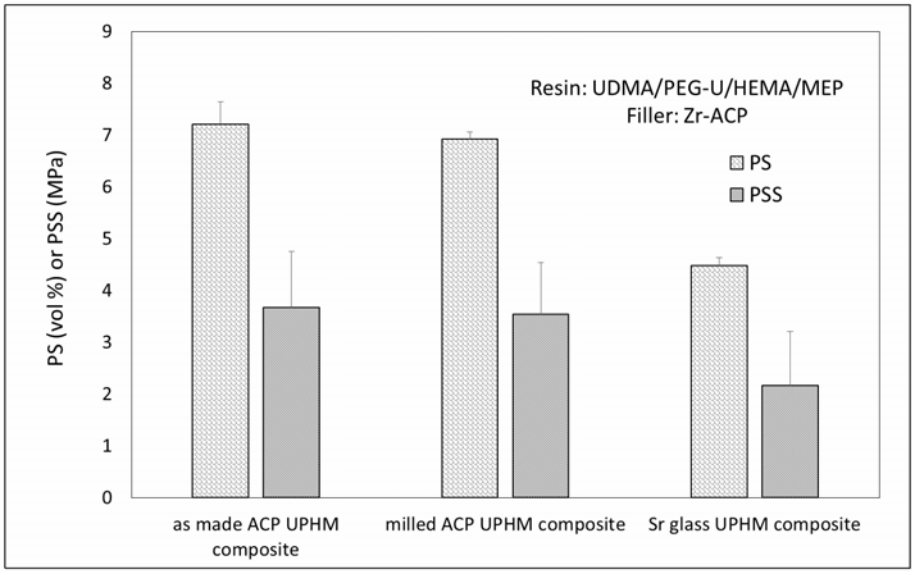

Fig. 7. PS and PSS of UPHM composites. Indicated are mean values + SD (n = 3).

Fig. 8. The maximum WS (after 3 months exposure to 75% RH or immersion in buffered saline at room temperature), the corresponding HE of ACP UPHM composites and supersaturation of the immersing solutions containing maximum concentrations of Ca and PO_4 ions released from the composites (non-applicable for copolymer and control group). Indicated are mean values + SD (n = 5).

consequently, a minimal likelihood of adverse cellular responses to these composites. In DC systems, a paste hardened within less than 10 minutes of mixing the CC components. Some degree of contraction occurred even before the sample was placed in dilatometer, making DC material unsuitable for measurement by this method. The PS measured in LC ACP UTHM composites [overall (7.0 ± 0.3) vol %] significantly exceeded the PS values of the glass-filled control [(4.4 ± 0.1) vol %]. However, normalizing PS values of the glass control to the resin/filler ratio of ACP composites brought them in line, with an average of 7.7 vol %. Similarly, the PSS developed in ACP UTHM composites [overall (3.7 ± 0.3) MPa] was higher than the PSS in glass-filled UTHM control [(2.2 ± 0.1) MPa]. These elevated PS values are significantly higher than the typical PS values reported for the commercial restoratives [(1.9-4.1) vol %] and flowable composites [(3.6-6.0) vol %]. At the same time the PS of ACP UPHM composites only slightly exceed the lower end values for the PS of adhesive resins [(6.7-13.5) vol %] [14]. This relatively high PS may, at least partially, be attributed to the intensified hydrogen bonding in UPHM resins with still relatively high content of HEMA (close to 17 mass %). The measured PSS values compare well with the PSS development in as-made binary UDMA/HEMA composites [63]. This would suggest that the actual stress resulting from the polymerization shrinkage in UPHM matrices was not elevated by the simultaneous inclusion of PEG-U and HEMA into polymer phase. The maximum WS values of specimens exposed to 75% RH, reached within two weeks, decreased in the following order: as-made ACP composite > (milled ACP composite, copolymer) > Sr-glass composite. The increases in mass of the specimens upon immersion in saline were 2.5 to 3 times compared to the corresponding specimens exposed to RH. The WS of immersed specimens decreased in the following order: (milled ACP composite, as-made ACP composite) > copolymer > Sr-glass composite. The HE of the specimens followed the same pattern. The kinetics of Ca and PO_4 release from both as-made and milled ACP UPHM composites were favorable and yielded solution supersaturations conducive to mineral re-deposition. A significant HE of ACP UTHM composites (up to 14 vol %) may be particularly useful in combating relatively high stress that develops in these materials. The potential benefits of HE have been reported by other researchers [64, 65].

To assess *in vitro* cytotoxicity of ACP/UPHM composites, their specimens were extracted in media and murine pre-osteoblasts (MC3T3-E1) and then cultured in extracts for 24 h. Extracts from a commercial endo-sealer (CES) were used as a reference. Medium without any extract and medium with added surfactant were used as a negative and a positive control, respectively. Morphology of cells exposed to different extracts was followed *in situ* by optical microscopy. Cells exposed to ACP/UPHM and CES extracts showed a contracted, spherical morphology (not shown here) and almost 2.5 times slower proliferation than the spread, polygonal cells in medium-only control. Significantly, similar morphological changes and proliferation rates were reported in hydrogel scaffolds designed for bone regeneration, in which pre-osteoblasts generated bone-like minerals [66]. The results of dehydrogenase activity (MTT assay) are shown in fig. 9. Based on these results, and regardless of the observed changes in cell morphology, our experimental ACP/UPHM composite is a viable candidate for the intended endodontic application (its cytotoxicity does not exceed the cytotoxicity of the commercial referent material).

To compare the apical micro-leakage (ML) of the ACP/UPHM sealer vs. the commercial material with the similar resin composition, we measured the penetration of the methylene blue dye solution after 72 h immersion at 37 °C. Root canals of single-rooted human teeth were treated step-wise with: 1) experimental PIDAA/PMDMA primer or Resilon primer, 2) experimental ACP/UPHM sealer or Resilon sealer, and 3) Gutta percha or Resilon filler. None of the eight treatment protocols provided highly desirable hermetic seal (Table 7).

While one-way ANOVA indicated no significant differences between treatments, multiple pair-wise analysis lead to the following conclusions: on average, root canals treated with ACP/UPHM sealer leaked less than those sealed with commercial products [(8.5 ± 3.4) mm vs. (10.3 ± 3.9) mm, respectively]. The treatments including experimental primer and ACP/UTHM sealer leaked the least distance from the apex. It is hard to explain generally the very high ML values seen in all groups tested. Inconsistency in root canal preparation should be excluded since a highly experienced endodontist was involved in its preparation. It is unlikely that the inconsistencies in application of primers, sealers and fillers lead to the extensive leakage since established protocols were strictly followed. It is, however, possible that for the teeth that were completely saturated with dye, during specimen

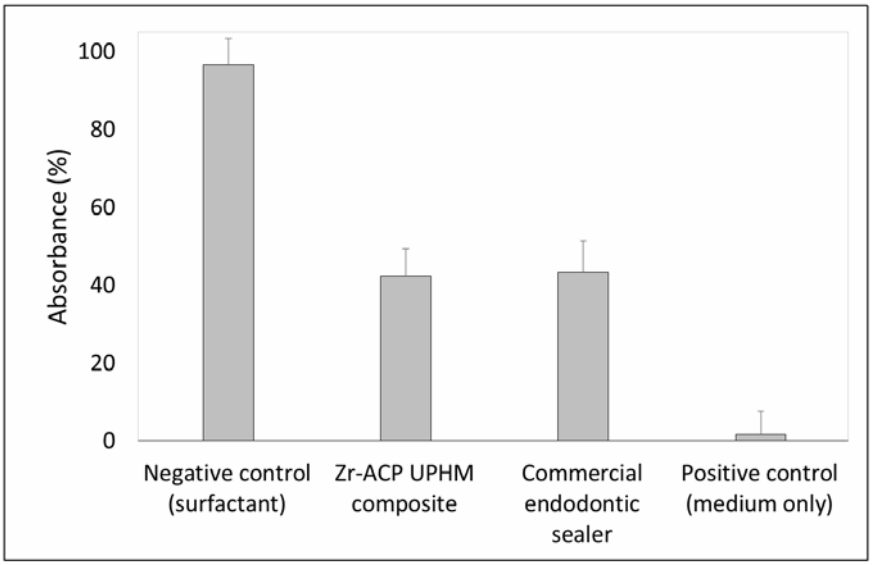

Fig. 9. MTT assay values (mean + SD; n = 3) for the experimental ACP UPHM endodontic composites, commercial control sealer and negative (medium + surfactant) and positive (medium only) controls.

Table 7. Micro-leakage (ML; mean + SD; n ≥ 5) of the sectioned root canal specimens primed with PIDAA/PMDMA or Resilon™ primer, sealed with the experimental Zr-ACP UPHM composite or Resilon™ sealer and filled with Gutta percha or Resilon™ filler. ML is expressed as a distance between the apical foramen and the 95% unstained dentin boundary. PIDAA/PMDMA solutions and the experimental ACP/UPHM composite were prepared in our Laboratory. Resilon™-Epiphany kits and Gutta percha were procured commercially.

Primer	Sealer	Filler	Micro-leakage (mm)
PIDAA/PMDMA	Zr-ACP UPHM	Gutta percha	5.5 ± 4.5
PIDAA/PMDMA	Zr-ACP UPHM	Resilon™	8.9 ± 3.5
PIDAA/PMDMA	Resilon™	Gutta percha	9.0 ± 1.3
PIDAA/PMDMA	Resilon™	Resilon™	9.7 ± 3.9
Resilon™	Zr-ACP UPHM	Gutta percha	10.0 ± 2.3
Resilon™	Zr-ACP UPHM	Resilon™	9.5 ± 3.1
Resilon™	Resilon™	Gutta percha	11.1 ± 5.5
Resilon™	Resilon™	Resilon™	11.3 ± 5.0

sectioning with the saw blade while cooling with water, the interior of the tooth was coated with the residual methylene blue. High ML values could also be explained by assuming that the majority of the teeth used in the study were collected from young patients whose root dentine is typically highly penetrable. However, since the teeth obtained from the local area dentists have no identifiers, our assumption cannot be corroborated. Our results contradict the reported ability of Resilon™ to provide an almost hermetic seal [55] and merit further evaluation of our experimental material. For that purpose, less error-susceptible methodology (fluid filtration and/or bacterial filtration) should be employed in future to re-confirm or dispute the findings of this study.

Leachability of unreacted monomers and the components of the photo-initiator system from UPHM copolymers and ACP composites were quantified by the ^{1}H-NMR, a valuable technique that provides both qualitative and quantitative information without a burden of a complex sample preparation and data interpretation. The results are shown in fig. 10. A (0.3-14.3) mass % and (0.3-10.4) mass % of initially incorporated monomers leached out from UPHM copolymers and ACP UPHM composites, respectively. Levels of CQ in the extracts were undetectable in both copolymers and composite series. The highest level leachability was detected with a photo-reductant, 4EDMAB (32.88 and 24.36 mass % in copolymers and composites, respectively). It is difficult to make a meaningful comparison of our leachability data with data reported in literature for several reasons. Firstly, the compositional makeup of the resins as well as the type and the load of fillers differ greatly from material to material. Secondly, researchers are employing a broad range of variable extraction conditions (solvent type, duration of extraction, ratio of specimen surface area/solvent volume, etc.). Thirdly, data are collected by using a variety of analytical methods. However, it is significant that the levels of unreacted HEMA detected in UPHM systems (0.03 mM) remained several orders of magnitude lower than the levels of HEMA typically released from restorative resins [(0.2-0.4) mM] and/or resin composites (up to 3 mM). This finding is particularly important having in mind the increased toxicity and adverse side effects reported for HEMA, which in the milieu metabolizes into methacrylic acid [67]. Furthermore, the level of the unreacted UDMA in UPHM formulations [(0.1-0.2) mM)] compares favorably with the concentrations of leached UDMA [(0.3-0.5) mM] reported for a wide range of the experimental UDMA/TEGDMA resins [68]. In conclusion, as a consequence of high DVC values attained in UPHM formulations, leachables from the UPHM specimens apparently did not exceed levels of leachables seen in commercial materials. In the complex UPHM polymer network, small molecular

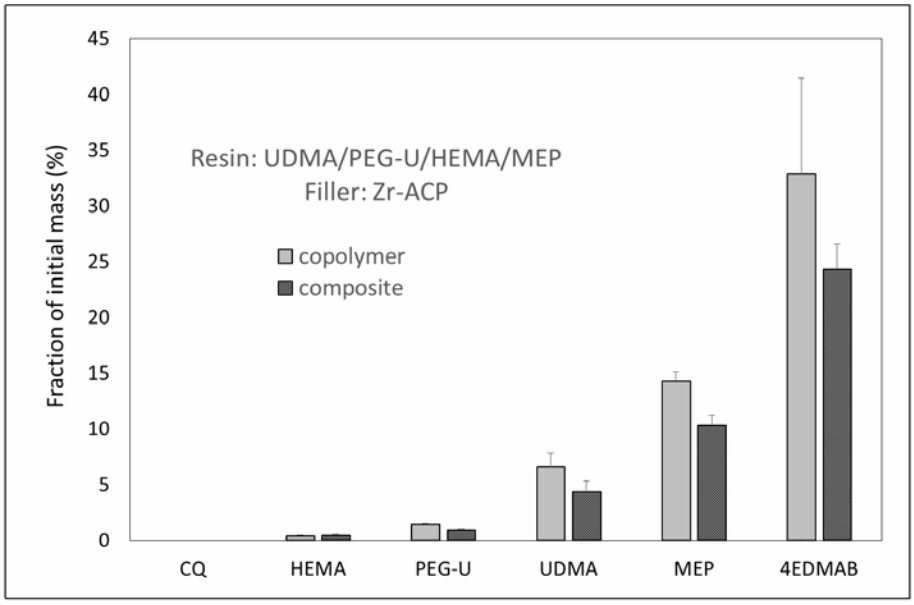

Fig. 10. Fractions of the initially incorporated monomers and photo-initiators detected in BHT-containing (0.01 mass % added to prevent secondary post-extraction polymerization) acetone extracts [7-day continuous extraction at 23 °C and magnetic stirring (32 rad/s)] of UPHM copolymers and their ACP composites. Indicated are mean values + SD; n = 3/group.

weight monomers such as HEMA, do not necessarily elute more than the higher molecular weight UDMA, as would be expected based on HEMA's mobility alone.

Quantitative remineralization studies

The remineralizing *in vitro* studies are considered to be a decisive proof that regeneration of lost tooth mineral indeed occurred upon the application of bioactive ACP composites. Quantitative remineralization efficacy studies were performed with the experimental ACP sealant (LC Bis-GMA/TEGDMA/HEMA/ZrDMA (BTHZ) resin; substrate – bovine teeth) and orthodontic adhesive (LC EBPADMA/TEGDMA/HEMA/MEP (ETHM) resin; substrate – human teeth). Results are summarized in fig. 11. Both types of experimental ACP composites showed superior remineralization activity compared with the controls. In experiments with bovine teeth, ACP sealant supported a significant mineral recovery (38.95% on average) while further demineralization took place in HAP/BTHZ and no-composite controls. In experiments with human teeth, remineralizing effect of the experimental ACP orthodontic adhesive was much stronger than that of F-releasing commercial control (14.38% vs. 4.41% mineral recovery, respectively). In contrast, no-composite control in ortho-adhesive series exhibited additional 55.65% mineral loss. In both studies, experimental design included accelerated acid attacks to account for effects of the prolonged service in more compressed timeframe. It is especially significant that in both bovine and human substrates, remineralization took place throughout the depth of the lesions rather than being confined to the regions near the surface. Such surface-restricted mineral recovery is typically seen in F-stimulated remineralization. In conclusion, both ACP/BTHZ and ACP/ETHM composites indeed provided necessary building blocks for restoration of tooth enamel. They could be used alone or in combination with F-releasing materials for both prevention and repair of carious lesions.

Groundwork for the future design of AMRE composites

Two cationic liquid QA monomers, bis(2-methacryloyloxy-ethyl) dimethylammonium bromide (IDMA-1) and 1,1'-bis[o-(2-methacryloyloxyethyl 2'methylphenylene) dimethylammonium bromide

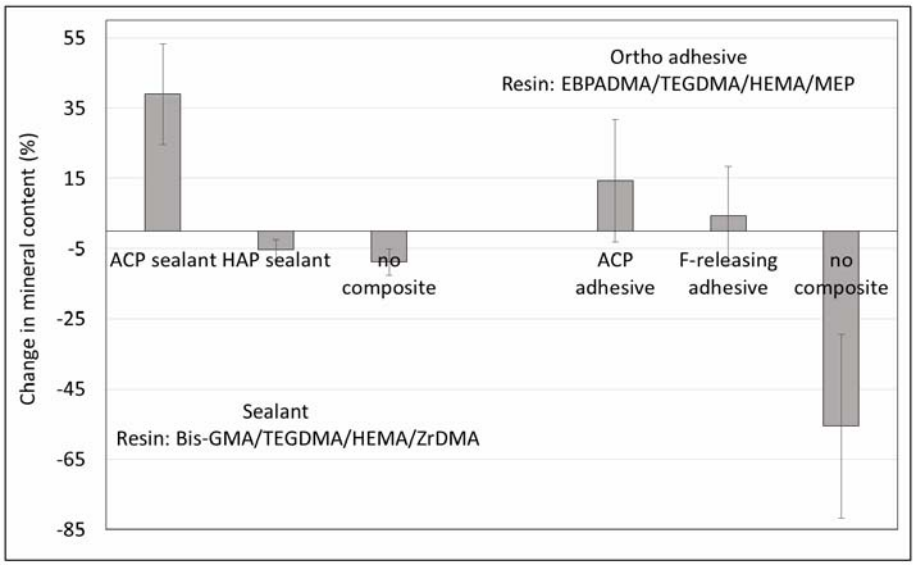

Fig. 11. Changes in mineral density upon specimen exposure to the pH-cycling regimen: ACP sealant (left) and orthodontic ACP adhesive series (right). Shown are mean Δ(ΔZ) values ± SD. Number of tooth specimens ≥ 4/group; number of analyzed microradiographic areas ≥ 8.

(IDMA-2) were successfully prepared and characterized by Fourier transform infrared spectroscopy. IDMA-1 and IDMA-2 both displayed new bands at 1089 cm^{-1}, 1048 cm^{-1}, 886 cm^{-1} and 858 cm^{-1}, and IDMA-2 also at 981 cm^{-1} and 712 cm^{-1}. These bands arise from vibrations of the NR_4^+ complexes (NR_4^+ groups have bands in the 1100 cm^{-1} to 450 cm^{-1} region [41]). Additional broad bands at 3412 cm^{-1} and 550 cm^{-1} were from hydrogen-bonded water. Proton-nuclear magnetic resonance spectroscopy (^{1}H-NMR) confirmed the assigned structures of IDMA-1 and IDMA-2. The AM action of IDMA-1 containing Bis-GMA/TEGDMA resins was assessed by measuring surface charge density, bacterial attachment, macrophage viability and enzymatic activity. Fluorescein binding to the cationic QA groups revealed significant increases in the levels of QA sites on the surfaces of polymers with higher IDMA-1 content. Polymers with 30% IDMA-1 had approximately 200 times more QA sites than other formulations. IDMA-1 reduced bacteria colonization at all tested concentrations. Also, bacterial morphology on the surfaces was altered on polymers containing 30 mass % IDMA-1. Image analysis (single fluorescent entities) confirmed that both density and surface coverage of *Streptococcus mutans* (Fig. 12) were significantly reduced in the presence of IDMA-1 compared to no IDMA-1 controls. There were, however, no significant differences among the IDMA-1 levels for either bacterial adhesion parameter.

Viability staining was used to assess macrophage density and viability (Fig. 13). The incorporation of 10% IDMA-1 significantly reduced cell density, and 20% and 30% IDMA-1 further reduced the density as compared to both 0% and 10% IDMA-1. Significantly cell viability was unchanged at 10% IDMA-1 but significantly reduced by 20% and 30% IDMA-1. Therefore, although the cell density was much lower with 10% IDMA-1 as compared to no IDMA control, the cell viability was not affected significantly. Macrophages on polymer disks (disk cells), as well as cells in the same wells as the polymer disks but adherent to the tissue culture polystyrene (TCPS) substrate, were evaluated independently (graphs not shown here). The results for the disk cell MTT activity agreed well with the viability results. At 10 mass %, IDMA-1 did not significantly affect the MTT activity while at higher IDMA-1 levels the MTT activity was significantly reduced. The results for the TCPS cells, however, showed no significant changes in

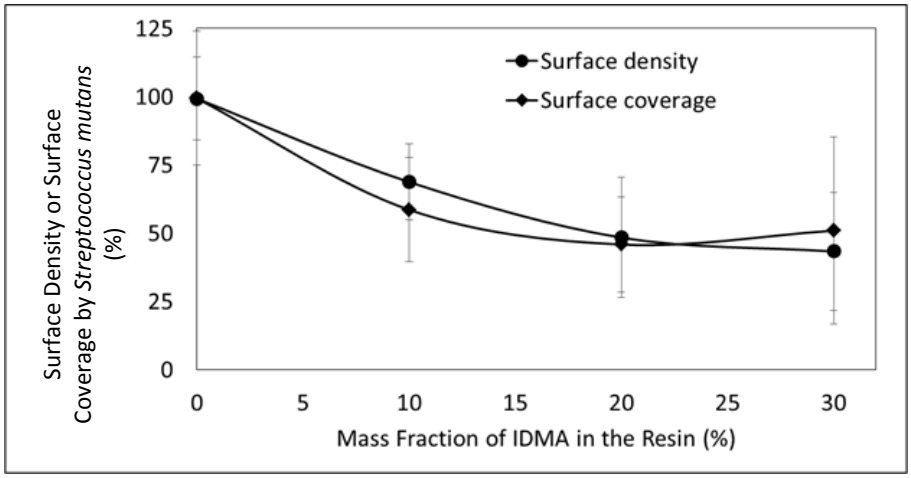

Fig. 12. Changes (mean value + SD) in relative surface density of *Streptococcus mutans* or relative surface coverage by bacteria as a function of IDMA-1 concentration in Bis-GMA/TEGDMA/IDMA (BTI) resin. Control density: (37,700 ± 5,700) objects/mm^2. Control surface coverage: (10 ± 2) %.

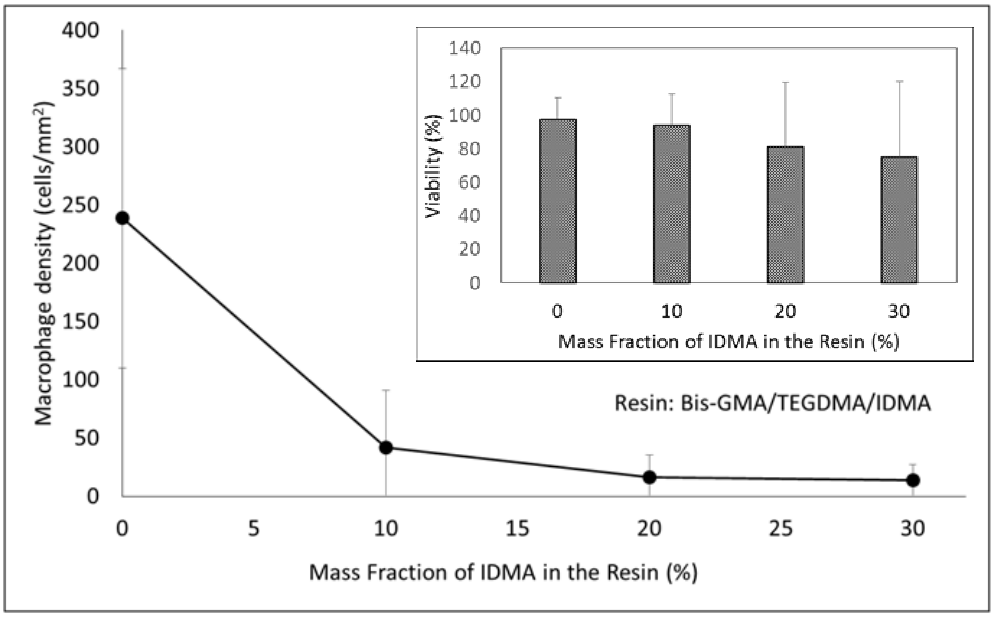

Fig. 13. Macrophage density and viability (inset) as a function of IDMA-1 concentration in BTI resin. Indicated are mean values + SD.

MTT activity as a result of the inclusion of IDMA-1. It is clear from this screening that a desired AM effect on pathogens and potential cytotoxicity of the AM agent to mammalian cells need to be carefully balanced. These aspects will strongly impact the design of a new family of AMRE composites.

CONCLUSION

In order to understand the structure-composition-property relationships in bioactive ACP-based polymeric materials, a battery of comprehensive physicochemical and mechanical tests applied to ACP fillers, copolymers and composites is required. These tests are particularly useful for identifying

the complex mechanisms that govern interactions between the ion-releasing, remineralizing filler and the polymer phase. Typically highly clustered ACP solids with a wide PSD can efficiently be converted into ACPs with narrower PSD. This is achieved by milling rather than ACP's surface modification *via* introducing additives during the spontaneous precipitation of ACP. The ACPs with narrower PSD yielded composites with more uniform filler distribution and improved mechanical properties while having no detrimental effect on their remineralizing ability.

Resins formulated for sealant, orthodontic and/or endodontic applications (Bis-GMA-, EBPADMA and UDMA-based, respectively) and their ensuing ACP composites typically attained high DVCs with the inclusion of the relatively high amounts [(10.0-29.2) mass %] of the mono-functional and highly-diffusive HEMA monomer into their resin phase. However, these high DVCs were accompanied by PS values exceeding those reported for the majority of commercial composites. This phenomenon can be partially explained by the much lower level of ACP filler in our experimental materials compared to the commercial controls (40 mass % vs. up to 85 mass %, respectively). In UDMA-based formulations, this high PS should be compensated by the high HE of the composites upon aqueous immersion.

Water-ACP filler and water-resin interactions are strong determinants of both mechanical integrity of the composites and their remineralization potential. Generally, ACP fillers, unlike silanized glass fillers, have no reinforcing ability and introducing ACP into resins typically diminished the mechanical performance of the composites compared to the corresponding polymers. The remineralizing potential of the composites was typically higher in EBPADMA- and UDMA-based polymers containing HEMA alone or HEMA plus PEG-U as co-monomers. The effect was attributed to the more open cross-linked network existing in these formulations as well as the hydrophilic character of HEMA leading to a higher water uptake and increased internal mineral saturation.

In vitro cytotoxicity evaluations that compare the experimental material with the representative commercial control are a good indicator of the material's appropriateness for the intended application. These tests need to be combined with the leachability studies and properly designed AM screening. Of particular importance would be assessing cellular toxicity of AMRE composites before the experimental material could be recommended for further evaluation in either animal models studies and/or clinical trials.

The findings of our continuing studies on bioactive ACP composites and the guidelines resulting from these studies have a potential to be used in future design of biodegradable, mineralization-supporting polymeric materials for the generalized bone repair.

DISCLAIMER

Certain commercial materials and equipments are identified in this article for the sole purpose of adequately defining the experimental protocols. In no instance does such identification imply endorsement and/or recommendation by the American Dental Association Foundation and the National Institute of Standards and Technology or that the material/equipment identified is the best available for the purpose.

ACKNOWLEDGEMENTS

The reported work was supported by the American Dental Association Foundation, the National Institute of Standards and Technology, and by the National Institute of Dental and Craniofacial Research (grants DE13169 and DE26122). Generous contribution of the monomers from Esstech, Essington, PA, USA is also gratefully acknowledged.

CONFLICT OF INTEREST STATEMENT

The authors declare no conflict of interest.

ABBREVIATIONS

AAS	:	atomic absorption spectroscopy sole
ACP	:	amorphous calcium phosphate
ADAF	:	American Dental Association Foundation
AES	:	atomic emission spectroscopy
AM	:	antimicrobial
am-ACP	:	as-made ACP
AMRE	:	antimicrobial & remineralizing

ANOVA : analysis of variance
BFS : biaxial flexure strength
BHT : butylated hydroxytoluene
Bis-GMA : 2,2-bis[p-(2'-hydroxy-3'-methacryloxypropoxy) phenyl]-propane
BPO : benzoyl peroxide
BT : Bis-GMA/TEGDMA resin
BTD : Bis-GMA/TEGDMA/ DEGMEMA resin
BTGd : Bis-GMA/TEGDMA/GDMA resin
BTGm : Bis-GMA/TEGDMA/GMA resin
BTH : Bis-GMA/TEGDMA/HEMA resin
BTI : Bis-GMA/TEGDMA/IDMA resin
BT4M : Bis-GMA/TEGDMA/4MET resin
BTMA : Bis-GMA/TEGDMA/A resin
BTMaA : Bis-GMA/TEGDMA/MaA resin
BTV : Bis-GMA/TEGDMA/VPA resin
CC : chemical cure
CQ : camphorquinone
CaP : calcium phosphate
CES : commercial endodontic sealer
CPP : casein phospho-peptide
D : diffusion coefficient
DC : dual cure
DEGMEMA : di(ethyleneglycol)methyl ether methacrylate
DHEPT : 2,2-dihydroxyethyl-p-toluidine
DeS : demineralizing solution
d_m : median diameter
DVC : degree of vinyl conversion
EBPADMA : ethoxylated bisphenol A dimethacrylate
4EDMAB : ethyl-4-N, N-dimethylaminobenzoate
FSP : anionic fluorosurfactant
ETHM : EBPADMA/TEGDMA/ HEMA/MEP resin
FTIR : Fourier-transform infrared
FTIR-m : FTIR microspectroscopy
$\Delta G0$: Gibbs free energy
GMA : glyceryl monomethacrylate
GDMA : glyceryl dimethacrylate
HAP : hydroxyapatite
HE : hygroscopic expansion
HEMA : 2-hydroxyethyl methacrylate
1850 Irgacure : bis(2,6-dimethoxybenzoyl)-2,4,4-triethylpentyl phosphine oxide & 1-hydroxycyclohexyl phenyl ketone
IAP : ion activity product
IDMA-1 : bis(2-methacryloyloxy-ethyl) dimethylammonium bromide
IDMA-2 : 1,1'-bis [o-(2-methacryloyloxyethyl 2'methylphenylene) dimethylammonium bromide
Ksp : thermodynamic solubility product
LSCM : laser scanning confocal microscopy
MaA : maleic acid
m-ACP : milled ACP
MA : methacrylic acid
MEP : methacryloyloxyethyl phthalate
4MET : mono-4-(methacryloyloxy) ethyl trimellitate
MTT : dehydrogenase activity assay
NIR : near-infrared
NMR : nuclear magnetic resonance
PAA : poly (acrylic acid)
PbTMBPO : phenyl-bis(2,4,6-trimethylbenzoyl) phosphine oxide
PEO : poly (ethylene oxide)
PIDAA : phenyliminodiacetic acid
PEG-U : poly(ethyleneglycol)-extended UDMA
PMDMA : adduct of pyromellitic dianhydride and HEMA
PSD : particle size distribution
PS : polymerization shrinkage
PSS : polymerization shrinkage stress
QA : quaternary ammonium
QS : quorum sensing
ReS : remineralizing solution
RH : relative humidity
SD : standard deviation
SBS : shear bond strength
SEM : scanning electron microscopy
S.m. : *Streptococcus mutans*
T : absolute temperature
TGA : thermogravimetric analysis
TEGDMA : triethyleneglycol dimethacrylate
UDMA : urethane dimethacrylate
UPHM : UDMA/PEG-U/HEMA/MEP resin
UV/VIS : ultraviolet/visible
VRC : Volpe research center
WS : water sorption
XRD : X-ray diffraction
ΔZ : mineral content of the lesion
$\Delta(\Delta Z)$: relative change in mineral content

REFERENCES

1. LeGeros, R. Z. 1991, Calcium Phosphates in Oral Biology and Medicine, Karger, Switzerland, 1.
2. Dorozhkin, S. V. 2011, Biomatter., 1(1), 3.
3. Dorozhkin, S. V. 2011, Biomatter., 1(2), 121.
4. Wang, L. and Nancollas, G. H. 2009, Chem. Rev., 108, 4628.
5. Zhao, J., Liu, Y., Sun, W. and Zhang, H. 2011, Chem. Centr. J., 5, 40.
6. Meyer, J. L. and Eanes, E. D. 1978, Calcif. Tissue Res., 25, 59.
7. Tadic, D., Peters, F. and Epple, M. 2002, Biomaterials, 23, 2553.
8. Boskey, A. L. 1997, J. Dent. Res., 76, 1433.
9. Weiner, S., Sagi, I. and Addadi, L. 2005, Science, 309, 1027.
10. Weiner, S. 2006, Bone, 39(3), 431.
11. He, G., Dahl, T., Veis, A. and George, A. 2003, Nature Materials, 2(8), 552.
12. Tsuji, T., Omima, K., Yamamoto, A., Ijima, M. and Shiba, K. 2008, PNAS, 105(44), 16866.
13. Beniash, E., Metzler, R. A., Lam, R. S. K. and Gilbert, P. U. P. A. 2009, J. Struct. Biol., 166(2), 133.
14. Skrtic, D., Antonucci, J. M. and Eanes, E. D. 2003, J. Res. Natl. Inst. Stand. Technol., 108(3), 167.
15. Pendrys, D. G. and Stamm, J. W. 1990, J. Dent. Res., 69, 529.
16. Reynolds, E. C., Cai, F., Cochrane, N. J., Shen, P., Walker, G. D., Morgan, M. V. and Reynolds, C. 2008, J. Dent. Res., 87(4), 344.
17. Reynolds, E. C. 1991, U.S. Patent 5015268.
18. Reynolds, E. C., Chain, C. J., Weber, F. L., Black, C. L., Riley, P. F., Johnson, I. H. and Perich, J. W. 1995, J. Dent. Res., 74, 1272.
19. Reynolds, E. C. 1997, J. Dent. Res., 76, 1587.
20. Skrtic, D., Eanes, E. D. and Antonucci, J. M. 1995, Industrial Biotechnological Polymers, C. G. Gebelein and C. E. Charraher (Eds.), Technomics Publ. Co., Lancaster, 393.
21. Skrtic, D., Antonucci, J. M. and Eanes, E. D. 1996, Dent. Mater., 12, 295.
22. Skrtic, D., Antonucci, J. M., Eanes, E. D., Eichmiller, F. C. and Schumacher, G. E. 2000, J. Biomed. Mat. Res. (Appl. Biomater.), 53, 381.
23. Antonucci, J. M., Skrtic, D. and Eanes, E. D. 1996, Hydrogels and Biodegradable Polymers for Bioapplications, R. Ottenbrite, S. Huang and K. Park (Eds.), ACS Symposium Series 627, 243.
24. Skrtic, D., Hailer, A. W., Takagi, S., Antonucci, J. M. and Eanes, E. D. 1996, J. Dent. Res., 75(9), 1679.
25. Ewoldsen, N. and Demke, R. S. 2001, Am. J. Orthod. Dentofac. Orthop., 120(1), 45.
26. Owers, J. M., Kim, H. B. and Turner, D. S. 1997, Seminars in Orthodontics, 3(3), 147.
27. Bergenholtz, G. and Spangberg, L. 2004, Crit. Rev. Oral Biol. Med., 15(2), 99.
28. Dorn, S. O. and Gartner, A. H. 1990, J. Endod., 16, 391.
29. Torabinejad, M. and Pitt Ford, T. R. 1996, Endod. Dent. Traumatol., 12, 161.
30. Dragoo, M. R. 1997, Int. J. Periodont. Res. Dent., 17, 75.
31. van Noort, R. 2013, Glass-ionomer Cements and Resin-modified Glass-ionomer Cements. An Introduction to Dental Materials (4th Ed.). Elsevier/Mosby, UK.
32. Torabinejad, M. and Chivian, N. 1999, J. Endod., 25, 197.
33. Weldon, J. K. Jr., Pashley, D. H., Loushine, R. J., Weller, R. N. and Imbrough, W. F. 2002, J. Endod., 28, 467.
34. Lee, Y. L., Lee, B. S., Lin, F. H., Yun, L. A., Lan, W. H. and Lin, C. P. 2004, Biomaterials, 25, 787.
35. Lee, Y. L., Lin, F. H., Wang, W. H., Ritchie, H. H., Lan, W. H. and Lin, C. P. 2007, J. Dent. Res., 86(6), 534.
36. Tanomaru, F. M., Figueiredo, F. A. and Tanomaru, J. M. 2005, Pesqui Odontol. Bras., 19, 119.
37. Imazato, S. 2009, Dent. Mater. J., 28(1), 11.
38. Pereira-Cenci, T., Cenci, M. S., Fedorowicz, Z. and Marchesan, M. A. 2009, Cochrane Database Syst. Rev., 8(3), CD007819.
39. Bodor, N., Kaminski, J. J. and Selk, S. 1980, J. Med. Chem., 23(5), 469.
40. Antonucci, J. M. 2012, US Patent No. 8,217,081 B2.
41. Antonucci, J. M., Zeiger, D. N., Tang, K., Lin-Gibson, S., Fowler, B. O. and Lin, N. J. 2012, Den. Mater., 28, 219.
42. Weng, Y., Howard, L., Guo, X., Chong, V. J., Gregory, R. L. and Xie, D. 2012, J. Mater. Sci.: Mater. Med., 23, 1553.

43. Gule, N. P., Bshena, O., de Kwaadsteniet, M., Cloete, T. E. and Klumperman, B. 2012, Biomacromolecules, 13, 3138.
44. Lönn-Stensrud, J. 2009, PhD Thesis, University of Oslo, Norway.
45. O'Donnell, J. N. R., Antonucci, J. M. and Skrtic, D. 2008, J. Comp. Mater., 42(21), 2231.
46. Murphy, J. and Riley, J. P. 1962, Anal. Chim. Act, 27, 31.
47. Skrtic, D., Antonucci, J. M., Eanes, E. D. and Eidelman, N. 2004, Biomaterials, 25, 1141.
48. Kirsten, A. F. and Woley, R. M. 1967, J. Res. Natl. Inst. Stand. Technol., 71C, 1.
49. Ban, S. and Anusavice, K. J. 1990, J. Dent. Res., 69(12), 1791.
50. Lu, H., Stansbury, J. W., Dickens, S. H., Eichmiller, F. C. and Bowman, C. N. 2004, J. Mater. Sci.: Mater. Med., 15, 1097.
51. Langhorst, S. E., O'Donnell, J. N. R. and Skrtic, D. 2009, Dent. Mater., 25, 884.
52. Teranaka, T. and Kolourides, T. 1987, Caries Res., 21, 326.
53. Chow, L. C., Takagi, S., Tung, W. and Jordan, T. H. 1991, J. Res. Natl. Inst. Stand. Technol., 96, 203.
54. Davis, C. H., O'Donnell, J. N. R., Sun, J. and Skrtic, D. 2011, Resin Composites: Properties, Production and Applications, D. B. Song (Ed.), Nova Science Publishers, USA, 55.
55. Bodrumlu, E. and Tunga, U. 2006, J. Contemp. Dent. Practice, 7(4), 045.
56. Simon, C. G. Jr., Antonucci, J. M., Liu, D. W. and Skrtic, D. 2005, J. Bioact. Compat. Polym., 20, 279.
57. Snedecor, G. E. and Cochran, G. W. 1989, Statistical Methods, 8th Edition, Iowa State Univ. Press, USA.
58. Montgomery, D. C. 1984, Design and Analysis of Experiments, 2nd Edition, John Wiley & Sons, USA, 209.
59. Neter, G., Kutner, M. H., Nachtsheim, C. J. and Wasserman, W. 1996, Applied Linear Statistical Models. 4th Edition, WCB/McGraw-HilI, USA, 683.
60. Wilson, A. D. and Nicholson, J. W. 1993, Chemistry of Solid State Materials. 3. Acid-base Cements. Their Biomedical and Industrial Applications, Cambridge Univ. Press, USA, 56.
61. Lee, S. Y., Regnault, W. F., Antonucci, J. M. and Skrtic, D. 2007, J. Biomed. Mater. Res.: Part B, 80B, 11.
62. Skrtic, D. and Antonucci, J. M. 2003, Biomaterials, 24, 2881.
63. O'Donnell, J. N. R. and Skrtic, D. 2009, J. Biomim. Biomater. Tissue Engn., 4, 1.
64. Momoi, Y. and McCabe, J. F. 1994, Brit. Dent. J., 176, 91.
65. Huang, C., Tay, F. R., Cheung, G. S. P., Kei, L. H., Wei, S. H. Y. and Pashley, D. H. 2002, J. Dent., 30, 11.
66. Chatterjee, K., Lin-Gibson, S., Wallace, W. E., Parekh, S. H., Lee, Y. J., Cicerone, M. T., Young, M. F. and Simon, C. G. 2010, Biomaterials, 31, 5051.
67. Durner, J., Walther, U. I., Zaspel, J., Hickel, R. and Reichl, F. X. 2010, Biomaterials, 31, 818.
68. Floyd, C. J. E. and Dickens, S. H. 2006, Dental Mater., 22, 1143.